ADSORPTION OF CHLORPYRIFOS FROM PESTICIDE WASTEWATER WITH ACTIVATED BENTONITE CLAY ADSORBENT

Abera Alemu Edae

A Thesis Submitted to the Department of Applied Chemistry

School of Applied Natural Science

Presented in Partial Fulfillment of the Requirements for the Degree of Master of Science in Applied Chemistry (Industrial Chemistry)

Office of Graduate Studies

Adama Science and Technology University

September, 2024

Adama, Ethiopia

Adsorption of chlorpyrifos from pesticide wastewater with activated bentonite clay adsorbent

Abera Alemu Edae

Advisor: Enyew Amare (PhD)

A Thesis Submitted to the Department of Applied Chemistry

School of Applied Natural Science

Presented in Partial Fulfillment of the Requirements for the Degree of Master of Science in Applied Chemistry (Industrial Chemistry)

Office of Graduate Studies

Adama Science and Technology University

September,2024

Adama, Ethiopia

APPROVAL SHEET

I, the advisor of the thesis entitled **"Adsorption of chlorpyrifos from pesticide wastewater with activated bentonite clay adsorbent"** and developed by **Abera Alemu Edae**; here by certify that the recommendation and suggestions made by the board of examiners are appropriately incorporated into the final version of the thesis.

Enyew Amare (PhD)

Major Supervisor	Signature	Date

We, the undersigned, members of the Board of Examiners of the thesis by **Abera Alemu Edae** have read and evaluated the thesis entitled **"Adsorption of chlorpyrifos from pesticide wastewater with activated bentonite clay adsorbent"** and examined the candidate during the open defense. This is, therefore, to certify that the thesis is accepted for partial fulfillment of the requirement of the degree of Master of Science in Applied Chemistry (Specialization in Industrial Chemistry).

Chairperson	Signature	Date
Internal Examiner	Signature	Date
External Examiner	Signature	Date

Finally, approval and acceptance of the thesis are contingent upon submission of its final copy to the Office of Postgraduate Studies (OPGS) through the candidate's Department Graduate Council (DGC) and School Graduate Committee (SGC).

Department Head	Signature	Date
School Dean	Signature	Date
Office of Postgraduate Studies, Dean	Signature	Date

DECLARATION

I hereby declare that this Master Thesis entitled **"Adsorption of chlorpyrifos from pesticide wastewater with activated bentonite clay adsorbent"** is my own work. That is, it has not been submitted for the award of any academic degree, diploma or certificate in any other university. All sources of materials that are used for this thesis have been duly acknowledged through citation.

_____	_____	_____
Name of student	Signature	Date

RECOMMENDATION

I, the major advisor of this thesis, hereby certify that I have closely advised/supervised the student while doing this thesis and read the thesis entitled **"Adsorption of chlorpyrifos from pesticide wastewater with activated bentonite clay adsorbent"** prepared under my guidance by Abera Alemu Edae submitted in partial fulfillment of the requirements for the degree of Masters of Science in Applied Chemistry (Industrial Chemistry). Therefore, I recommend the submission of revised version of the thesis to the department following the applicable procedures.

_____	_____	_____
Major Advisor	Signature	Date

DEDICATION

This M.Sc. thesis is dedicated to the glory of God, to my beloved families, to my Mother Abebech Wake, to my daughter and son Amensis and Hawinet Abera and especially thanks to my wife Addis Tadelle, whose advice, support, and prayers, helped me all along the right way. They will always be in my heart.

ACKNOWLEDGMENT

I want to start by sincerely thanking the Almighty God for providing me with the courage and poise I needed to complete my studies in a safe and sound manner. It is truly impossible to put into words how grateful I am, but I will do my best to show my appreciation to select individuals. Despite the fact that this study reflects my accomplishments, I would like to acknowledge the several persons who have greatly benefited me. Above all, I want to thank my adviser, Dr. Enyew Amare, for his unwavering support, counsel, proofreading, and scientific contribution on this research project. I appreciate the vital assistance provided by the Quality Assurance Department Laboratory member at the Adami Tulu Pesticides Processing Factory.

Additionally, I am grateful to the following individuals for their contributions to the scientific success of this thesis: Ato Demeke Tasfaye from Adama Science and Technology University (ASTU) for TGA-DTA and XRD characterization; Prof. Yonas Chebude from Addis Ababa University (AAU) for FT-IR characterization; Ato Leta from Adama Science and Technology University (ASTU) for SEM characterization; and Ato Biniyem Abebaw from the Chemical and Construction Inputs Industry Research Development Center Laboratory for XRF characterization. Last but not least, I would want to sincerely thank my family, who are all well-wishers and helped me finish this thesis.

LIST OF ABBREVIATIONS

AAU	Addis Ababa University
ASTU	Adama Science and Technology University
AWCFPS	Actual Weight of Chlorpyrifos Standard
AWCFPT	Actual Weight of Chlorpyrifos Technical
FTIR	Fourier Transform Infrared
SEM	Scanning electron microscopy
TGA	Thermal gravimetric analysis
DTA	Differential thermal analysis
USEPA	United State Environmental Protection Agency
UV-VIS	Ultraviolet Visible
WWTP	Wastewater Treatment pond
XRD	X-ray diffraction
L.O.I	Loss on Ignition
XRF	X-ray florescent
APPF	Adami tulu pesticides processing factory
CPF	Chlorpyrifos
AB	Activated bentonite
RB	Raw bentonite
PHpzc	pH Point of zero charge
HPLC	High performance liquid chromatography
HHPs	Highly hazardous pesticides
POP	Persistent Organic Pesticides

TABLE OF CONTENTS

LIST OF FIGURES

LIST OF TABLES

ABSTRACT

Chlorpyrifos is an organophosphate insecticide that reaches water sources for multiple reasons, and people who use water from nearby sources are exposed to chlorpyrifos. The adsorption of chlorpyrifos insecticides by using the low-cost 5% sodium bicarbonate activated bentonite was investigated at different adsorbent dose, pH, contact time, contaminant concentration and regenerative ability via batch experiment method. The raw and activated bentonite were characterized by fourier transform infrared spectrometry (FT-IR), X-Ray Diffractometer (XRD), differential thermal gravimetry (DTG), X-ray fluorescence spectrometer (XRF) and scanning electron microscopy (SEM). The results of the XRD showed that the raw bentonite is composed of montmorillonite, quartz, muscovite, hematite, feldspar and cristobalite. X-ray and FTIR data confirmed that 5% sodium bicarbonate activation affects both the octahedral and the tetrahedral sheets. The results of the analysis by X-ray fluorescence spectrometer (XRF), showed that, presence of silica, alumina, magnesium, calcium and iron as major constituents, along with traces of sodium, potassium, titanium, sulfur and phosphorus in the form of impurities. The differential thermal analysis curve confirms that the sample did not undergo phase changes and is thermally stable up to 500 ℃. High performance liquid chromatography (HPLC) was used to identify and analyze the chlorpyrifos insecticides. The activated bentonite demonstrated a 99.1% chlorpyrifos removal efficiency, a capacity of 49.3 mg/g, at an optimum condition at pH 6, 100 ml/L initial concentration, 40 minutes contact time and 2 g/L adsorbent dose and excellent reusability for four cycles. The Langmuir's isotherm model was found the best fit, with the high value 0.9894 of correlation coefficient (R^2) and with the monolayer adsorption capacities 3.659 mg/g of chlorpyrifos. The amount of adsorbed at equilibrium was (Qe, cal) obtained for first and second order kinetics were (19.49 and 36.65 mg/g) respectively. The kinetic result obtained at the equilibrium of (Qe, cal) and high correlation coefficient (R^2 = 0.9976) value of pseudo second order model was suggesting that more of the adsorption process might be chemical sorption. The findings outlined the potential of the newly developed AB was able to reduce chlorpyrifos in the adami tulu pesticides processing factory wastewater pond from 0.974 mg/L to 0.09 mg/L with 90.76% removal efficiencies.

Keywords*: Chlorpyrifos, Insecticide ,Activated bentonite, Characterization, Adsorption, batch experiment method.*

1. INTRODUCTION

1.1. Background of the study

Water shortage and quality deterioration, along with the ever-increasing population would, be great challenges facing many countries worldwide. Along with that, water resources are polluted with industrial, domestic, and agricultural waste (Elzakey et al., 2023). Agricultural fertilizer and pesticides significantly improve crop yields and quality by protecting against pests. The increasing use of pesticides in agriculture and domestic activities is increasingly contaminating water resources (Suciu & Capri, 2009). Several works have recently reported that the presence of agricultural pesticides in water bodies is due to both diffuse from aerial applications and point sources, and indeed the latter may be the largest influence on water quality at the catchment and regional scale. Point sources include sites where pesticide formulations are diluted, where pesticide sprayers are loaded, storage of empty containers, or where occasional spills occur, discharge of industrial wastewaters control, leaching and run-off from agricultural and forest lands; and discharges from greenhouses where none of the implementation of good agricultural practices and the installation of simple depuration systems (Elzakey et al., 2023, Joshi et al., 2023, Johnson et al., 2015). A certain portion of the applied amount may be deposited outside the target area, such as on untargeted soil, plant, and water surfaces. A key potential route to surface water is from spray drift. For plant protection, many pesticides are sprayed very close to surface water. This causes spray drift, shown in Figure 1 deposition ranging from 0.3% to 3.5% of the normal field (Hussain & Asi, 2008).

Figure 1: Pesticides spray drift (Hussain & Asi, 2008).

The persistent nature of organophosphorus pesticides and their translocation from agricultural land as runoff or as irrigation return flow can cause pesticide residues in water sources. However, the persistent nature of the pesticides is of great concern due to their bio-accumulative nature and toxic biological effects on wildlife and humans (Hossain et al., 2015). On the other hand, pesticides have become universal contaminants found in all segments of the environment and create many hazards to the environment and human health (Derbalah et al., 2013). The frequent high concentrations (over guideline values) of pesticides detected are due to the extensive utilization of pesticides in the agricultural fields. Specifically, organophosphorus pesticides contaminated various ecosystems around the world and caused adverse effects to millions of people, with over 200,000 deaths annually. Furthermore, improper disposal and overuse of pesticides have added large amounts to water and soil environments. The emerging contaminant chlorpyrifos is one of the organophosphorus insecticides used in agricultural fields that reaches water sources for multiple reasons, and people who use water from nearby sources are exposed to chlorpyrifos (Joshi et al., 2023). By 2050, about 6 billion people will suffer from the scarcity of clean water (Elzakey et al., 2023).

Consequently, human exposure to these pesticides' residues might occur throughout the food chain the leading to various adverse impacts (Elzakey et al., 2023). Chlorpyrifos has been used continuously at very high concentrations around the world, causing environmental elements to be contaminated in a number of ways. This has been substantiated by reports showing chlorpyrifos concentrations in groundwater, freshwater lakes, rivers, streams, city hurricane drains, rain, fog, marine sediments, sumps, sloughs, and even in air, as well as both solid and liquid food samples from rural and urban areas (Joshi et al., 2023). The wastewater samples collected from El-Khairy agricultural drainage, which receives agricultural and domestic wastes, were analyzed for pesticide residues via gas chromatography-mass spectroscopy (GC–MS) system and results uncovered the presence of ten pesticides ranging from 0.0817 to 28.162 µg/l, and the predominant pesticide was chlorpyrifos (Elzakey et al., 2023).

Additionally, significant health concerns have been found in chlorpyrifos and endosulfan, which are strongly adsorbed and slowly degrading pesticides, were found in nearly all surface

and groundwater samples, with maximum concentrations in surface water of 8 µg/L for chlorpyrifos and 3 µg/L for endosulfan.The chlorpyrifos was found in the groundwater in the dry and rain phases. They are resistant to microbial degradation. It suggests that this chemical is adsorbed to the soil in the aquifer near the wells. This was expected since the degradation is slow for this chemical (Sishu et al., 2022). In 32 soils and 64 drinking water samples from 16 cocoa farms in the Dormaa West District of Ghana. Four organophosphorus residues were detected in the soil and water samples at varying concentrations. The organophosphorus residues recorded in the water samples were chlorpyrifos, diazinon, and pirimiphos-methyl 0.01–0.05, 0.01–0.04 µg/L and (0.01–0.03 µg/L respectively. All organophosphorus pesticide residues recorded in the water samples from the various sites within the various distances were below and within their respective WHO MRLs for drinking water except chlorpyrifos and diazinon which exceeding their WHO MRLs. Chlorpyrifos and diazinon concentrations in drinking water that exceeded their respective WHO MRLs may pose health hazards to farmers' households and the communities (Fosu-Mensah et al., 2016). The concentrations of detected organophosphorus pesticides ranged from 0.070 to 2.95 mg/L either at the intake or outlet points for drinking water of different water purification plants. With respect to the detected compounds in all sampling sites during the two sampling times, the detection frequency was abundant in the following order: chlorpyrifos, dimethoate, dichlorvos, fention, mevinphos, phorate, tetrachlorovinphos, malathion, coumaphos, merphos, trichloronate and sulprofos, respectively (Derbalah et al., 2013).

In general, among 12 samples, 10 samples were found contaminated with pesticides. 2, 4-D and chlorpyrifos were often determined at different concentrations. Chlorpyrifos was also detected in four tested samples, and concentrations ranged from 3.27 to 9.31 µg/L (Pluangklang & Rangsriwatananon, 2021). Residues of many pesticides, among them chlorpyrifos, have been detected in wastewater, groundwater, surface water, and soil. The detected concentrations of chlorpyrifos in both surface and ground water are in the range of 0.13-0.24µg/L. The concentration also stretches between the values of 0.1-107 mg/L (Anupam et al., 2022). Therefore, residues of pesticides are extensively dispersed in drinking waters, ground waters, and soils during application by spraying. People and animals exposed to chlorpyrifos may suffer serious consequences, whether directly by inhalation or indirectly

through skin, ocular contact, and other sources such as dissolved water. Chlorpyrifos is known for its ability to act as cytotoxic, genotoxic, re-productivity toxic, and immune toxic to both humans and animals. It has been documented that exposure of birds and aquatic ecosystems to low concentrations of chlorpyrifos caused severe toxicity to these organisms (Qurie et al., 2016). Residues of pesticides have significant environmental impacts on aquatic ecosystems and mammals. In general, chlorpyrifos exposure in children can cause permanent neuronal developmental abnormalities such as autism and attention deficit hyperactivity disorder (ADHD) (Joshi et al., 2023). The effects of a pesticide can be either acute or chronic. Examples of acute health effects include stinging eyes, rashes, blisters, blindness, nausea, dizziness, and diarrhea. Examples of known chronic effects are cancers, birth defects, reproductive harm, neurological and developmental toxicity, immune toxicity, and disruption of the endocrine system. Environmental pollution with pesticides is one of the most serious problems facing the world due to their potential toxicity, high persistence, and slow degradation (Johnson & Kumar, 2015).

Some pesticides are highly toxic, non-biodegradable, and persist in the environment for a very long period of time. Chlorpyrifos had the longest half-life of over a year and a surface water concentration of chlorpyrifos was highly toxic to fish (Sishu et al., 2022). Chlorpyrifos is the most used organophosphate insecticide, although it is considered hazardous and has been included on the list of priority substances in the water policy established by the European Community (Suciu & Capri, 2009).

The World Health Organization (WHO) Maximum Residue Limit (MRL) value of pesticides is 0.05 µg/L for drinking water (Fosu-Mensah et al., 2016) and as established by the European Union of Drinking Water Directive (EU/1998), to the quality of water intended for human consumption, the maximum allowable concentrations in drinking water guidelines is 0.1 µg/L for single pesticide and 0.5 µg/L for the sum of all pesticides. Thus, the removal or treatment of this pesticide (OPPs) from contaminated water is pertinent (Baharum et al., 2020, Ivanova et al., 2016).

Therefore, cleaning water resources through the implementation of proper remediation methods is extremely needed (Elzakey et al., 2023). Several methods are available for pesticide removal, such as solid-phase extraction, photocatalytic degradation, photo-Fenton, flocculation, chlorination, ozonation and adsorption. An increasing attention has been focused on adsorption techniques due to their efficiency in the removal of pollutants from aqueous solution (Senthilkumaar et al., 2010). Adsorption is a simple and convenient method for the removal of compounds compared to other physical, chemical, or biological technologies. It also involves low investment in terms of both initial cost and land required (Pluangklang et al., 2021). Removal of pesticides from aqueous solutions is performed by the various adsorbents, such bio adsorbents and inorganic adsorbents as, activated carbon, polymeric adsorbents, and activated bentonite clay, are used to remove pesticides from aqueous solutions (Samadi-Maybodi et al., 2023). The special properties of bentonite (hydration, swelling, viscosity, and thixotropy) and plausible mechanism/interaction for the adsorption/absorption of pesticide onto the clay, the wide versatility, naturally abundant, low cost, eco-friendly, accessible (Farghali et al., 2020) and wide, and their propensity to be chemically and physically modified, are the major driving forces behind the technological needs that make it a valuable material for a wide range of uses and applications (Abdullahi et al., 2017, Fisseha et al., 2017).

In this study, 5% sodium bicarbonate activated bentonite “AB” was used as a low-cost material for the removal of chlorpyrifos pesticides from aqueous solution. The aim of this work was to study the sorption properties of activated bentonite (AB) while removing chlorpyrifos insecticides from aqueous solutions. The efficiency of chlorpyrifos adsorption by the “AB” was investigated by various physiochemical analysis.

1.2. Statement of the problem

By controlling pests like insects, weeds, and rodents that are detrimental to agricultural or hort icultural plantings, pesticides help produce a sufficient supply of food for the growing global population.More than a thousand distinct types of chemicals are active against pests, and at le ast 2.5 million tons of pesticides are used annually worldwide.Pests, plant diseases, and weeds may still account for almost 40% of the world's potential food output. Therefore, there is no denying that using pesticides increases agricultural output. On the other hand, excessive pesticide use has several negative effects on both human health and the environment by

destroying food, soil, air, and surface and groundwater quality. In particular, organophosphorus pesticides have harmed ecosystems worldwide and resulted in about 200,000 deaths and 26 million cases of pesticide poisoning every year (Elzakey et al., 2023, Johnson & Kumar, 2015).

These days, numerous researchers have proposed a variety of alternative low-cost adsorbents, including natural clays like bentonite, kaolinite, and sepiolite, industrial and agricultural by-products, and other adsorbents like activated carbon and zeolites that have been used to remove pesticides and their derivatives from aqueous solutions. Because of its huge surface area and superior adsorption ability, activated carbon is a useful adsorbent for the elimination of organic pesticides. However, its widespread application is limited due to high cost and regeneration problems. Recently clay adsorbents have received attention because of their availability, low cost, and environmental friendly. The removal performance of chlorpyrifos inseciticeds in Adami tulu pesticide processing factory wastewater treatment pond, that contains 0.974 mg/L has investigated. Thus, it is essential to remove chlorpyrifos insecticide from chlorpyrifos polluted wastewater. The removal of chlorpyrifos from aqueous solution has been achieved through chemical, physical and biological methods. In recent time, adsorption using activated bentonite clay appears the most economical method because of its inexpensiveness, easy working principle, and high pollutant uptake capacities (Leena et al., 2017). This study will describe the activation of raw bentonite clay by easily and low cost method as adsorbent to remove chlorpyrifos from chlorpyrifos polluted wastewater.

1.3. Objective

1.3.1. General objective

The overall objective of this study was the adsorption/removal of chlorpyrifos from aqueous solutions by sodium bicarbonate activated bentonite.

1.3.2. Specific objectives

The specific objectives of this study are:

- To activate and characterize the sodium bicarbonate activated bentonite by using different characterization techniques like XRD, FTIR, XRF, and SEM.
- To investigate the adsorption capacity and removal efficiency of activated bentonite for chlorpyrifos insecticides from aqueous solution.
- To determine the effects of initial chlorpyrifos concentration, pH, adsorbent dosage and contact time on the adsorption performance of sodium bicarbonate activated bentonite.
- To study the adsorption mechanism through adsorption isotherm and kinetics.
- To evaluate regeneration ability of activated bentonite adsorbent.

1.4. Significance of the study

Chlorpyrifos has been used continuously at very high concentrations around the world, causing contaminated water resources in a number of ways both diffuse from aerial applications and point sources. Chlorpyrifos is known for its ability to act as cytotoxic, genotoxic, re-productivity toxic and immune toxic to both human and animals. Also exposure in children can cause permanent neuronal developmental abnormalities such as autism and attention deficit hyperactivity disorder (ADHD) and cause severe toxicity to birds and aquatic organisms. In general, chlorpyrifos pesticides can cause serious problems for the environment and several health problems for humans and animals. This study is expected to provide a method to remove chlorpyrifos insecticides that pose serious health and environmental hazards using activated bentonite a simple, cost-effective, and environmentally friendly adsorption method. It reduces the acute or chronic effects of water pollution due to toxic substances from chlorpyrifos insectides that can cause serious problems for the humans and animals. The research will be essential for other researchers and academicians to perform additional investigation by expanding this examination to other persistent organic pesticides.

2. LITERATURE REVIEW

2.1. Bentonite clay

Bentonite is a term that was first used to designate particular, highly colloidal, plastic clay found near Fort Benton in the Cretaceous beds of Wyoming, USA, with the dominant content of smectite minerals, usually montmorillonite which is the determinant factor in the clay's properties, named after the deposits in Montmorillon, France (Fisseha et al., 2017). Bentonites are clay stones, mainly formed by hydrothermal alteration of volcanic rocks. They are mostly composed of clay minerals from the smectite family. Montmorillonite, as the most common smectite, Smectites are a group of clay minerals with a 2:1 phyllosilicate structure. The tetrahedral and octahedral sheets present isomorphic substitutions of mainly Si (IV) for Al (III) and of Al (III) for Mg (II), respectively, so that an excess of negative charge is generated in the structure that constitutes a permanent layer charge, so the electrostatic force between the charged layers and the exchangeable cations in the interlayer zone is diffuse. The major mineral in bentonite is montmorillonite, hydrated sodium, calcium, magnesium, aluminum silicate. The sodium, calcium, and magnesium cations are interchangeable giving the montmorillonite a high ion exchange capacity (Cuevas et al., 2022). The presence of an interlayer space and the moderate magnitude of the laminar charge in its structure facilitate the entry of hydrated cations to neutralize the structural negative charge, and for this reason, smectite acts as a cation exchanger. These structural characteristics explain at the molecular level one of the most important properties of montmorillonite: its swelling capacity in water. Besides, montmorillonite is a mineral with a very small crystal size, typically made up of laminar layer stacks of 10 nm in thickness × 50 nm in section, which facilitates its contact with an external solution. Bentonites have a wide variety of industrial uses: foundry molds for the steel industry, bentonite-drilling muds for use in excavation, binder for pellets, and as a construction material resistant to the passage of water, etc (Cuevas et al., 2022).

The bentonite phyllosilicate groups that occur as silicate layers in a three-phase crystalline structure that promotes intrinsic characteristics. The clay mineral surface poses a negative charge due to the edge hydroxyl groups, giving rise to intermolecular hydrogen bonds with the hydrophilic medium. Furthermore, the presence of inorganic cations can stabilize its

silicate layers by Van der Waals forces. Additionally, the surface Brønsted, Lewis acid sites, and ion exchange sites are the main reasons for bentonite clay's excellent absorptivity.

Figure 2: Raw bentonite (Hussain & Asi, 2008).

Its igneous origin, with a high specific surface area of 20 to 130 m^2/g, has found numerous applications in ceramics, adhesives, catalysts, desiccants, cosmetics, pharmaceutical industries, as well as water and waste water treatment (Shattar et al., 2020).

2.2. Occurrences and chemical composition of bentonite clay

The structure of bentonite clay is formed by repetition units along the basal axis, which consists of two types of sheets: one Al octahedral sheet placed between two Si tetrahedral (Fig. 2). Tetrahedral sheets consist of corner-linked tetrahedral with oxygen in the corners and cations (T) in the center. The dominant cation is Si^{4+}, but Al^{3+} is substituted for it frequently, up to half of the Si. Fe^{3+} is substituted for Si^{4+} occasionally; the tetrahedral rests on a triangular face and shares all three oxygen's with three other tetrahedral of the hexagonal symmetry. Octahedral sheets consist of edge-linked octahedral with OH in the corners and cations (R) in the center. The cations are usually Al^{3+}, Mg^{2+}, Fe^{2+}, or Fe^{3+}, but all other transition elements and Li are possible. The octahedral sheets can be described as composed of two planes of closest-packed hydroxyls with cations occupying the octahedral sites between the two planes.

The isomorphous substitution of Al^{3+} for Si^{4+} in the tetrahedral layer and Mg^{2+} for Al^{3+} in the octahedral layer results in a net negative surface charge on the bentonite. These imbalanced charges in the interlayer space are balanced by the dominant cations, typically Na^{+}, K^{+}, Mg^{2+},

and Ca^{2+}. These cations are exchangeable due to their loose binding, and this leads to the high cation exchange capacity of bentonite.

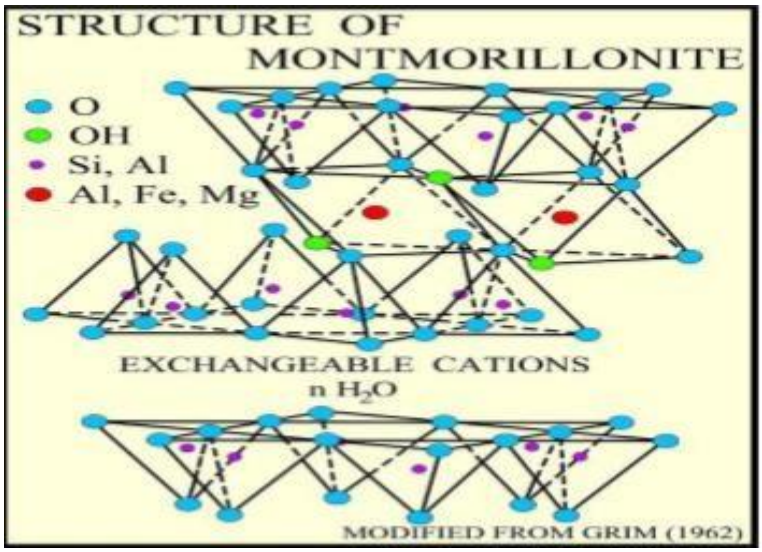

Figure 3: Diagrammatic sketch of the structure of montmorillonite (Leena et al., 2017).

Calcium montmorillonite and sodium montmorillonite are the most important clay minerals in the smectite group. The main structural difference between calcium and sodium montmorillonite is the water layer. Calcium montmorillonite possesses two water layers in the interlayer position while sodium montmorillonite has only one water layer. With only one water layer in the interlayer position, sodium montmorillonite has significantly different properties than calcium bentonite. Sodium montmorillonite has a much higher swelling capacity and viscosity than calcium montmorillonite. The unique feature of bentonite is that the particle may develop a permanent and variable charge on the different surfaces of the same particle. The siloxane ditrigonal cavity of the phyllosilicate siloxane surfaces could form a localized permanent negative charge as a result of isomorphic substitutions in their internal crystalline structures. The magnitude of this permanent negative charge does not depend on the pH of a solution. In contrast, the edges of Fe/Al oxides have surface reactive groups with amphoteric properties resulting from the protonation and dissociation of Al–OH and Si–OH superficial functional groups, which are positively charged under acidic conditions or negatively charged under basic conditions. Depending on the nature of their origin, bentonite may contain a variety of accessory minerals or non-clay impurities in addition to montmorillonite. These minerals may include quartz, feldspar, calcite, and gypsum. The presence of these minerals could impact the industrial value of the deposit, reducing or

increasing its value depending on the application. In particular, bentonite purification via mechanical, thermal, and chemical treatments often turns out to be necessary. Among these, chemical modifications by acid activation are usually expected to produce pronounced implications (Shattar et al., 2020).

Table 1: Chemical composition of Ethiopian bentonite (Wasse Bekele et al., 2014)

Locality	Oxide (weight %)											
	SiO_2	Al_2O_3	Fe_2O_3	CaO	MgO	Na_2O	K_2O	MnO	TiO_2	P_2O_5	H_2O	LOI
Gewane	61	11.5	6.9	0.7	2.6	1.3	1.1	0.1	1	-	10	4.8
Warssia	49	13.4	8.71	3.87	2.79	1.1	1.31	0.1	1.61	-	-	-
Gidicho	60.8	10.9	13.5	0.9	1.3	2.2	1.1	0.16	1.09	-	2.3	7.7

Bentonite clay resources are found in the Afar and Oromia regions of Ethiopia. They are easily accessible as they are located near the main road. The main occurrences in Afar are located at:Ledi, Gewane, Hadar, and Warseiso. The total resources in the Afar region are estimated to be 170 million tons (Fisseha et al., 2017, Tadesse et al., 2022).

2.3. Activation method of bentonite

2.3.1. Mechanochemical activation

Mechanochemical activation (MCA) is a process able to induce structural disorder, amorphisation, and increased chemical reactivity in the material treated by intensive grinding. The MCA is a simple method to apply, especially when done by milling. The entire process is characterized by small energy requirements and low processing temperatures, which reduces costs, and increases environmental friendliness. Processing of bentonite by MCA led to the damage of the crystal structure and the generation of almost an amorphous material, especially when using long grinding times. The loss of crystallinity led to the formation of a solid silica gel. Optimized process parameters can result in an amorphized structure of clay minerals being obtained already after 20 minutes of fine grinding. In the MCA process, amorphisation also appeared to destroy the bonds between the tetrahedral and the octahedral layers montmorillonite, ripidolite, or kaolinite) because MCA caused the formation of new more reactive surfaces. In addition to decreased crystallinity and particle size, MC processing of montmorillonite or kaolinite, has shown interesting changes as e.g. creation of amorphous

oxides of Mg, increased content of Fe^{3+} cations compared to Fe^{2+} in processed montmorillonite, improvement of the DC conductivity in both kaolinite and montmorillonite (Tole et al., 2019).

2.3.2. Thermally activation

The main effects of the calcination method are on the particle size and the specific surface area of the clay. The rotary kiln and furnace oven (also known as "soak") methods tend to increase the particle size and decrease the specific surface area, whereas these effects are not observed for flash calcination. These phenomena are enhanced with increasing calcination temperature, with particle size increasing due to agglomeration and specific area subsequently decreasing if sintering takes place at higher temperatures. Since this coarsening effect decreases the available surface area for dissolution, the calcination temperature should be kept as low as possible (Khalifa et al., 2020). Heat treatment of less than 450°C significantly changes the surface properties of bentonite; it improves porosity by increasing mesopore volume, the number of surface adsorption sites, and the number of siloxane groups present while decreasing the number of hydroxyl groups (Pluangklang et al., 2021).

2.3.3. Acid activation

Acid activation is a modification technique that aims to produce partial dissolution of the adsorbent to enhance the adsorptive properties, surface crystallinity, functionalities, specific surface area, and selectivity for different adsorbates. It is usually conducted for the total dissolution of undesired non-clay components and controlled attack, particularly on the octahedral layer, to generate a more acidic Si-rich phase. Magnesium and, to a lesser extent, aluminium are the elements most readily removed during acid modification. Similarly, bentonite activation is a complex phenomenon that involves the substitution of exchangeable cations, Al^{3+}, Mg^{2+}, and Fe^{2+} against protons from the octahedral sheet, resulting in the improvement of bleaching effectiveness, greater hydrophobicity and porosity structure, a strongly protonated clay mineral surface, an increase in specific surface area from the original 20–130 m^2/g to more than 200 m^2/g, and generating higher affinity for organic molecules such as 2.4-D and chlorpyrifos. In this sense (Shattar et al., 2020, Leena, 2017).

The type and concentration of the acid effect on modified clay were used for the removal of organic substances. Furthermore, mild conditions can stabilize clay structures, and the effect of heat used in the modification process was also promoted for the removal of organic

compounds. Thus, combining both treatments to modify bentonite rather than solely with heat or acid, and considering the sequence of each treatment in the modification of bentonite in order to optimize active sites for the adsorption of pesticides such as atrazine (basic), diuron (non-ionic), 2,4-D (acidic), and paraquat (cation) in aqueous media (Pluangklang et al., 2021).

2.3.4. Sodium activation of bentonite

Calcium bentonite is the most commonly available clay in the world including Ethiopia. Permeability and other properties of bentonite can be improved by additives or activation includes exchange activation, grinding or pulverizing which is designed primarily to improve dispersion. The properties of calcium bentonite can be modified to some extent by processing, e.g. to remove impurities or to incorporate additives or by activating the bentonite. Additives may include dispersants, flocculants or gelling agents and are usually designed to improve performance and manageability of bentonite suspension. In this sense, the present work was carried out to shed light on the feasibility of 5% sodium bicarbonate activated bentonite (AB) for the adsorptive treatment of chlorpyrifos agrochemical insecticide the second generation of industrial and agricultural pesticide contaminants from the aqueous solution(S. K. Saleh et al., 2015,Unnithan et al., 2017).

2.4. Physical-chemical properties of chlorpyrifos pesticides.

Chlorpyrifos is an organic thiophosphate form of agrochemical insecticide and plays as acetylcholinesterase and cholinesterase) inhibitor. Owing to its non-polar nature, chlorpyrifos has a low solubility in water and a great tendency to partition from aqueous into organic phases in the environment. The IUPAC name for chlorpyrifos is O, O-diethyl. O-3, 5, 6-trichloro-2-pyridyl phosphorothioate(World Health Organization, 2004).

Table 2: Physico-chemical properties of pure chlorpyrifos

Structural Formula	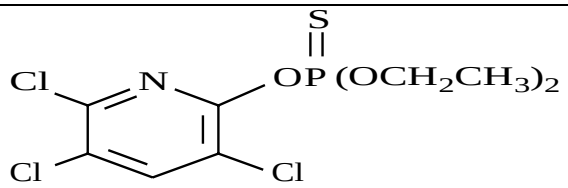
Common Name (ISO)	Chlorpyrifos
Chemical Name	O,O-dimethyl O-3,5,6-trichloro-2-pyridinyl phosphorothioate
IUPAC name	*O,O*-dimethyl O-3,5,6-trichloro-2-pyridyl phosphorothioate
Chemical Family	Organophosphates
Molecular weight	322.5 g/mol
Empirical formula	$C_7H_7Cl_3NO3PS$
Appearance	colorless crystals to tan colored crystalline solid
Melting point	46.0 ℃
boiling points	160 ºC
Relative density	1.642 at 23 ℃
Odour	mild mercaptan odour
Stability	Stable under normal storage conditions
Solubility at 20 ºC	In water at 20 ℃ distilled water: 2.74 mg/L

2.5. Environmental Fate of Chlorpyrifos

It is an emerging environmentally noxious waste. The environmental fate of chlorpyrifos consists mostly of sorption-desorption to soil matrix, scattering into deeper soil layers, percolating into groundwater, plant uptake, volatilization, and deprivation. Many studies have shown that the environmental fate of chlorpyrifos is heavily influenced by its persistence, movement, and bioavailability, which is a complicated procedure, influenced by numerous variables other than its characteristics. The physical and chemical interface among the chemicals and other elements defines the fate of chlorpyrifos in the environment. Chlorpyrifos is dispersed throughout the environment and undergoes many changes, including oxidation, photolysis, photo-degradation, photo-mineralization, biotransformation, and associated

metabolic processes in living things. Adsorption, volatilization, leaching, runoff, absorption, and degradation are the primary routes. Despite their low concentration, this contaminant puts a major risk to environmental and human health due to their incomplete removal during the treatment (Kumar et al., 2023). USEPA2 included the chlorpyrifos compound in 400 listed products that can be advertised for many industrial, agricultural, and domestic pest control applications. In 2007, chlorpyrifos was recognized as the most widely used organophosphorus pesticide in the United States, with an annual use of around five million kg active ingredients (AI) (Kumar et al., 2023). Reported that the annual global quantity of chlorpyrifos used between 2002 and 2006 was 25 million kg AI, with 98.5% of the quantity used in agricultural fields. The most intense quantities of chlorpyrifos are used in the crops, cotton, corn, almonds, fruit trees, oranges, and apples. Excess quantities of pesticides lead to contamination of the surrounding soil, and it is difficult to separate chlorpyrifos from soil. Chlorpyrifos has an intermediate vapor pressure and under some conditions, its volatility is a significant mechanism of dissipation. Therefore, instead of water-dissolved chlorpyrifos, soil-bound chlorpyrifos from eroding soil is more likely to be the cause of chlorpyrifos discharge into water from soil. Chlorpyrifos remains in the soil for approximately 60 to 120 days and then degrades into 3, 5, 6-trichloro-2-pyridinol, which is further broken down into organochlorine chemicals and carbon dioxide due to microbial activity (Joshi et al., 2023).

2.6. Conventional technologies for the removal of chlorpyrifos from water

2.6.1. Chemical treatment techniques

2.6.1.1. Advanced Oxidation Processes

Advanced oxidation processes (AOPs) involve the use of hydrogen peroxide (H_2O_2) oxidizing agents with combination of O_3, and/or UV treatment and react with array of substances to remove harmful persistent organic pollutants (POPs) from water. AOPs are environmentally friendly chemical techniques that can degrade organic contaminants into harmless products that neither transfer contaminants from one phase to another nor produce massive amounts of sludge. Furthermore, this technique has various advantages, including rapid reaction rates that lead to less retention time compared to other conventional treatment techniques, and it does not require a large area for processing the needed flow rates for the system. However, various drawbacks can also be highlighted, including its high operating and maintenance costs. It also

has a complex chemistry tailored to specific contaminants, which requires skilled personnel to design the system. Nowadays, AOPs are considered high-efficiency physical-chemical processes due to their thermodynamic viability and are capable of producing deep changes in the chemical structure of the contaminants via the participation of free radicals. These species, mainly hydroxyl radicals ($HO^{\bullet}$) and sulphate ($SO^{\bullet}_4$), are of particular interest because of their high oxidation capability. One disadvantage of hydrogen peroxide (H_2O_2) is that under certain conditions, such as high temperature, H_2O_2 can rapidly decompose into hydrogen and oxygen. Hydrogen peroxides is considered a hazardous chemical which requires secondary containment, and handling precautions, as well as special operator training (Kamalanathan et al., 2016).

2.6.1.2. Chlorination

Chlorination is a chemical water treatment method used to put limits on bacterial growth in wastewater, which helps in controlling odor and taste. Chlorination has the advantage of being cheap and easy to implement. However, pre-chlorination can cause the oxidation of micro-contaminants into the intermediates by products that could be more toxic and less removable than the patent compounds. A study investigating chlorination as a pre-treatment method for pesticides showed a negative impact. As a result, chlorination is used prior to filtration using powdered activated carbon with coagulation sedimentation filters (PAC-CSF) (I. A. Saleh et al., 2020). The result showed that the pre-chlorination of OPP oxidized them into more toxic axons that are hard to remove by PAC-CSF, as shown in figure 4. Therefore, water contaminated with OPPs should not be treated by chlorination in order to avoid removal complications. They have studied chlorination for the treatment of an initial concentration of 100ng/L of nine different organophosphate pesticides from water, including methyl parathion. The result showed that chlorination has led to the formation of oxon and other oxidation products that are stable in water and require further toxicity tests (I. A. Saleh et al., 2020).

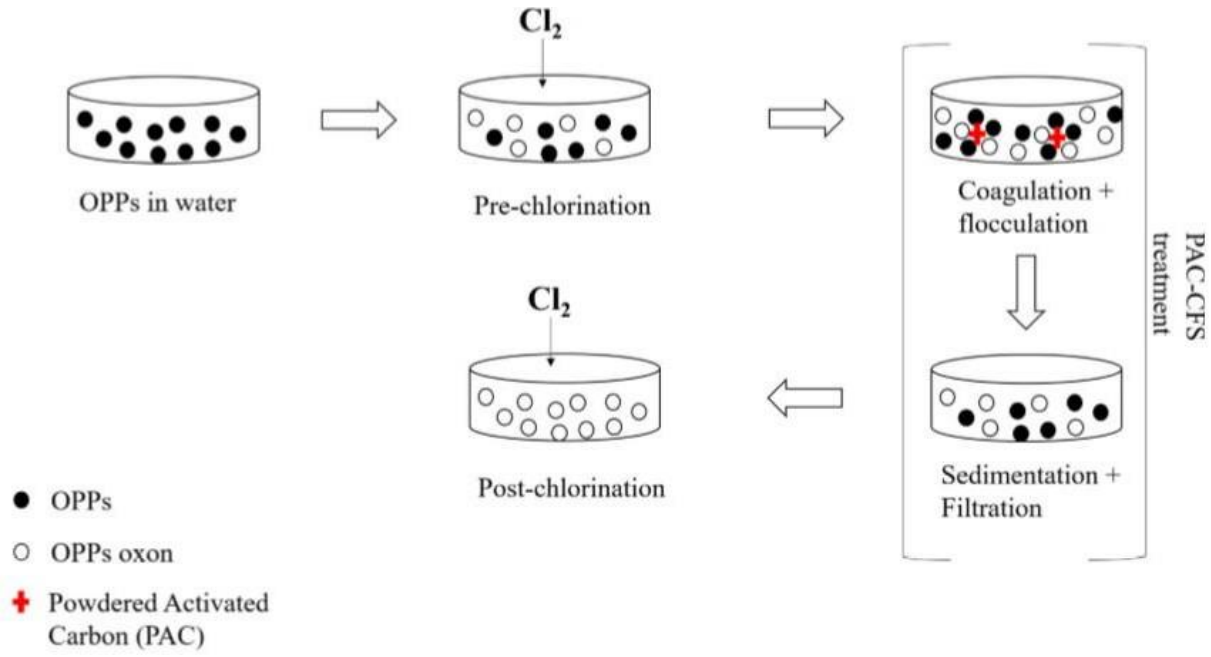

Figure 4: The schematic of chlorination as a pretreatments technique for removal of organophosphorus pesticides (OPPs) from water (I. A. Saleh et al., 2020).

2.7. Biological treatment method

2.7.1. Bioaugmentation

This method uses isolated microbes for the degradation of pesticides. The pesticides are quickly metabolized and converted to products with lower toxicity under aerobic and anaerobic conditions. Certain pesticides are capable of being degraded by certain bacterial strains as their sole nutrient or carbon source. Such microbial reactions are known as mineralizing because of the large amount of carbon dioxide released during metabolism.

Dichlorodiphenyltrichloroethane, normally resistant to biodegradation, has been reported to have been metabolized in an anaerobic microbial culture, followed by an aerobic one. Reported that bacteria isolated from soil were capable of degrading 83%–93% of the organophosphorus pesticide, monocrotophos and a 96% reduction in isoxathion from the organophosphorus pesticides by bacteria isolated from turf green soil. The triazophos bacteria are capable of degrading 33.1% to 95.8% of pesticides. The downside of such a method is the establishment of the microbes in the presence of other microbial populations present in the

contaminated soil. Also noted that the population of the introduced bacteria may be reduced due to susceptibility to predation or starvation (T. Al Hattab & E. Ghaly, 2012).

2.7.2. Membrane bioreactor (MBR)

MBR is one of the latest technologies in wastewater treatment. It combines membrane filtration techniques with biological treatment. Despite its high efficiency, it is worth noting that this technique requires high energy, in addition to the cost of antifouling techniques needed to keep it functioning**.** The action of bioremediating bacteria in a MBR is limited due to the antibiotic added to the pesticide to avoid bacterial spoilage of crops. Therefore, pesticide-rich wastewater is also rich in antibiotics (I. A. Saleh et al., 2020)**.**

2.8. Physical treatment techniques

2.8.1. Membrane Filtration

Membrane filtration techniques are being widely used in wastewater treatment plants. Depending on the membrane types and the target contaminants, filtration can be implemented at any stage during water treatment. The type of filtration depends on the membrane cut-off size. Nano-filtration membranes with pore sizes between 10^{-2} and 10^{-3}µm are ideal for the removal of bacteria, viruses, and large organic molecules have evaluated four different types of polyamides nano-membranes for the filtration of dimethoate (an organophosphate insecticide) and atrazine. Both pesticides are recognized as public health concerns and have their maximum limit in water set by the world health organization (WHO). The lab-scale experiment assessed the filtration capacity of the tested membranes in which the amounts of contaminants were tested by HPLC. The best membrane among the four twisted membranes was named NF90, with a retention rate of 85% for dimethoate and 95% for atrazine; the initial concentrations of the pesticides were tested at 2 and 20 mg/L, respectively. In another study, nano-filtration was proven in another study to separate the herbicide glyphosate from saline wastewater. They used the interfacial polymerization technique to synthesize a thin-film composite (TFC) poly (piperazine amide) nanofiltration membrane and investigated the effect of triethylamine (TEA) as an accelerator on the performance of the membrane. Results indicated that adding TEA to the membrane improved the rejection and water flux as it was higher compared to the other membranes, where the rejection of diazinon and water permeability increased from 95.2% and 22 $L/m^2/h$, respectively, for the unmodified membrane to approximately 98.8% and 41.56 $L/m^2/h$ for the TEA modified membrane. A

significant improvement was indicated in poly (piperazine amide) TFC nanofiltration membranes for the removal of pesticides (I. A. Saleh et al., 2020).

Membrane processes play a significant role in wastewater treatment, and the use of nanoreactive membranes and advanced filtration materials helps in water recycling and desalination. Recent studies have demonstrated that membrane technology can be successfully applied to purify wastewater released by textiles, leather, food, electronics, and dairy industries, as well as municipal wastewater. Since conventional treatment methods are not able to remove compounds such as organic pollutants and nutrients to the sufficient level required for the effluents to meet the standard quality. The common types of membrane processes used in water purification systems include microfiltration, ultrafiltration, and nanofiltration for water treatment processes (Kamalanathan et al., 2016)(Figure. 5). This will highlight the nanofiltration and different types of membrane processes used in the wastewater treatment plant (WWTP).

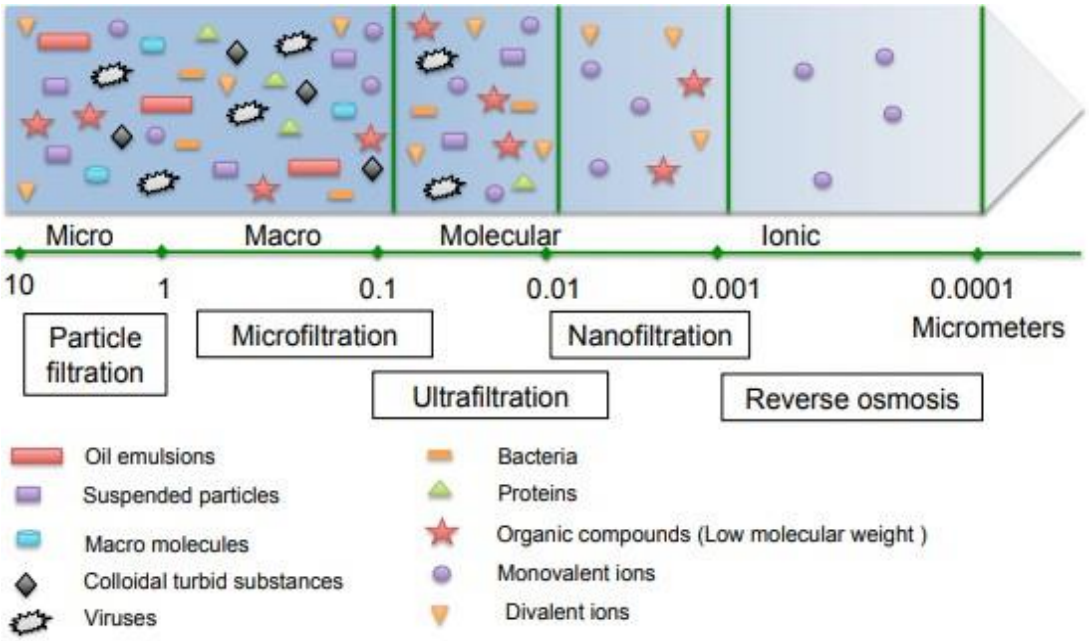

Figure 5: Size dependent filtration methods (Scale: Micro particle range, Macro molecular range, Molecular range, Ionic range (Saleh, Zouari, and Al-Ghouti 2020)

2.8.2. Adsorption treatment process

Adsorption is a simple and convenient method that is showing very effective results in purifying some of the environmentally and publicly stressful contaminants from water compared to other physical, chemical, biological, or nanotechnologies (Farghali et al., 2020). It also involves low investment in terms of both initial cost and land required. The effectiveness of the adsorbent depends on the number of sites available, porosity, surface area, and the possible interaction with the target contaminants. Many successful trials were documented due to the high porosity and high surface area of activated carbon. Due to their high production cost, agricultural wastes, synthetic polymers, and bio-adsorbents such as sludge waste, fermentation waste, yeast, and seaweed are used as sources of activated carbon. Furthermore, inorganic adsorbents such as clay and graphene are of interest in water treatment techniques because of their low cost. Although experimental conditions such as pH, initial load, and total volume of water treated were varied, the percentage helps in comparing the efficiency of the different adsorbents. Adsorption removal of organic contaminants has proven to be a cost-effective option in wastewater treatment, with the only drawback being that the contaminants are not mineralized during the process. The process leaves the solid adsorbent waste loaded with contaminants that must be incinerated or treated before being discarded (I. A. Saleh et al., 2020).

Various solid substrates offer good adsorptive properties, including zeolites, activated carbon, fly ash, mesoporous silica, and clay minerals, which are applied in the removal of organic contaminants from water. Bentonite clay is abundantly available, an important, low-cost source of montmorillonite, and exhibits excellent adsorption capacities as well as high cation exchange capability (CEC), minerals not only in Ethiopia, but their deposits are widespread all over the world. The hydration of these inorganic cations causes the clay mineral surface to be hydrophilic. These cations are easily replaced by both organic and inorganic cations, accounting for the unique hydrophilic, tumescent, and adsorption properties of montmorillonite (Abdullahi et al., 2017).

Adsorption is a simple and convenient method that is showing very effective results in purifying some of the environmentally and publicly stressful contaminants from water compared to other physical, chemical, biological, or nanotechnologies (Farghali et al., 2020).

In the finding solution by the adsorption method the examples figure 2 show steps of the problem-to-solution process that involves removing chlorpyrifos using various

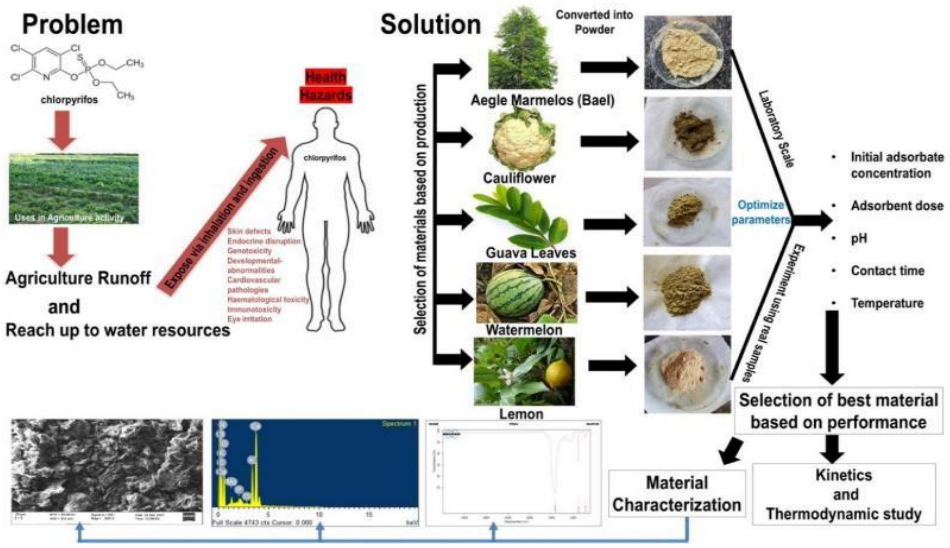

Figure 6: Steps of the problem-to-solution process that involves removing chlorpyrifos using various bio adsorbents (Joshi et al., 2023)**.**

3. MATERIALS AND METHODS

3.1. Materials

3.1.1 Chemical and reagent

The following chemicals were used: Chlorpyrifos, (analytical standard, with purity 98.4% from Syricit China National pesticides Quality Inspection Testing Center (Shenyang), chlorpyrifos technical grade with purity 97% (Tianjin Bohai chemical import and export Company) was purchased from a chemical supplier. N-hexane, anhydrous sodium chloride (Merck, Germany), hydrochloric acid, sodium hydroxide, sodium bicarbonate (99.5%), HPLC grade acetonitrile (Sigma-Aldrich, Steinheim, Germany ≥99%), acetic acid and water that were used.

3.2.1. Equipments and Instruments

The equipments and instruments used for characterization of adsorbents during this research work were, X-ray fluorescence spectrometer (XRF, EDX3- 600H China), Fourier Transform-Infrared Spectrometer (FT-IR) (model 65FT-IR, PerkinElmer,USA), X-Ray Diffractometer, Shimadzu Corporation Japan, XRD-7000, Scanning Electron Microscope (SEM) (JCM-6000PLUS Bench Top SEM, JEOL, Japan), differential thermal gravimetry (DTG) (Shimadzu co., DTG-60H, South Korea Japan), and HPLC equipped with UV-Vis detector (Perk Elmer AUG, USA), Milli-Q water purification apparatus with model:ZROQ00800 S/N F1DA45767C, (Ireland), Rotary evaporator (model, buchi/R-210Switzerland), Karl fisher (Mettler Toledo , model 103 A, Switzerland), halogen rapid moisture analyzer (Mettler Toledo HR83, Switzerland) ,digital electronic balance (kern 770 P/N ED 021830, Germany), muffle furnace (MF2015, Italy), pH meter (model Mettler-Toledo GmbH), oven (Thermostatic oven Yamato model: DKL610C S/N: J1108007, Japan), Ultra sonic water bath, with time & temperature control (Auto science AS5150AD ,China), laboratory milling apparatus (DFT-50 max-25000 r/min China, Eppendorf centrifuge (5702 model, SA), separating funnel (Duran, Germany),syringe filter head (0.45 µm pore size), Solvent filtration system (Kontes , USA), mortar and pestle, glass rod, pipettes, spatulas, Erlenmeyer flask, ISO -3310-1 laboratory test sieve (Endecotts ltd London England serial no.417145) standard sieve, volumetric flask, pycnometer, graduated cylinder and other than these sample collection materials (Poly ethylene plastic bags and Glass bottles), different sizes of beakers were used for different activities.

3.2. Methods

3.2.1. Preparation of chlorpyrifos Stock and working Solutions.

A stock solution of both chlorpyrifos for standard reference and sample solution were prepared by taking the actual weight 25.5mg and 1031mg using the equation (1) and (2) was dissolved with acetonitrile in 500 and 1000 mL volumetric flasks respectively. Other samples for all experiments were prepared by diluting the stock solution with Milli –Q purified water to the predetermined concentration.The solution was degassed for 15 min in an ultrasonic bath and stored in a refrigerator at 4 ^{0}C. A stock solution was used for preparation of chlorpyrifos concentration that used for calibration curve and adsorption test with different pesticide concentrations (0.001– 250 mg/L) by serial dilution method in appropriated volumetric flasks with the Milli-Q purified HPLC grade water using the equation (3). The standard series solutions were prepared from the mother (stock C1) solution by using serial dilution method. Finally HPLC equipped with a UV-Vis detector was used to measure the concentrations of chlorpyrifos solutions.

AWCFPS = (Weight of standard × Purity of standard)/100 ---------- (Eq.1)

AWCFPT = (Weight of technical grade × Purity of technical grade)/100 ----------(Eq.2)

Where: AWCFPS and AWCFPT (x) were the actual weight of the standard and technical grade chlorpyrifos respectively.

The serial dilution of the working standard and sample solution of chlorpyrifos was prepared by using the following formula.

$C_1V_1 = C_2V_2$ ---------- (Eq.3)

Where: C_1 represents mother solution, V_1 represents volume of mother solution, C_2 and V_2 were concentration and volume to be prepared (Samadi-Maybodi et al., 2023,Suciu et al., 2009,Joshi et al., 2023).

3.2.2. Collection and Pretreatment of Bentonite

The natural bentonite used in the study was collected from different locations/directions of Gewane deposit (figure 7) Afar regional state, North Eastern Ethiopia.

Figure 7: Picture showing bentonite deposit at Gewane area, Afar region, Ethiopia (Wasse Bekele et al., 2014).

The raw bentonite was dispersed in deionized water several times to be cleaned from impurities. The suspension was allowed to stand for 24 hr to settle the impurities. The supernatant was decanted and centrifuged. Then clay settled at the bottom of the container by allowing standing for 24 hr was collected and dried in the oven at 105 °C for 24 hr. The dried bentonite cooled to room temperature in the desiccators was grinded under a sieve mesh size of 45μm and labeled as purified bentonite "RB" stored in air tight capped amber glass bottle and stayed in the desiccators for the preliminary adsorption test (Unnithan et al., 2017).

3.2.3. Preparation of activated bentonite

3.2.3.1. Sodium bicarbonate activated bentonite (AB).

The "RB" was milled and homogenized with 2, 3, 4, 5, and 6% sodium bicarbonate ($NaHCO_3$). The mixture was pulverized by laboratory milling apparatus with 25000 r/min and dispersed into deionized water and stirred for 2 hr by using a mechanical stirrer at 560 rpm and allowed to stand for 24 hr. After that it was separated into two phases with a bentonite part at the bottom and clear water suspension at the top which was removed by using a vacuum pump. After collecting bentonite remaining impurity formed at bottom of the beaker and sieved under a sieve mesh size of 45μm to retain the oversized particles such as quartz clay and other impurities in the bentonite which is not settled at the bottom the suspension was then centrifuged at 2500 rpm for 15 min and washed three times with

deionized water. Thereafter, the residue was dried at 105 ± 2 °C for 24 hr using a laboratory thermostatic oven. The dried bentonite cooled to room temperature in the desiccators was grinded again by using laboratory milling apparatus and sieved under a sieve mesh size of 45μm and labeled as activated bentonite "AB_2, AB_3, AB_4, AB_5, and AB_6" stored in air tight capped amber glass bottle and placed in desiccators until further used (Unnithan et al., 2017).

3.3. Physical characterization of raw and 5% sodium bicarbonate activated bentonite clay

3.3.1. Moisture content

The moisture content of raw and 5% sodium bicarbonate activated bentonite clay were determined by drying approximately 1g of bentonite clay at 120 and 110 °C in a rapid halogen moisture analyzer and in a thermo constant heat oven until the mass became constant. Then after cooling in desiccators, the moisture content was calculated using the equation (4) (Leena et al., 2017).

$$M = \frac{w1 - w2}{w1} \times 100 \quad \text{..... (Eq. 4)}$$

Where: M (%): percentage of moisture in the sample

W1: weight of wet sample (grams)

W2: weight of dry sample (grams)

3.3.2. PH determination

The pH value of raw and 5% sodium bicarbonate activated bentonite were measured directly using a glass electrode pH meter. The pH of raw and activated bentonite was determined by using soaked 5g of clay in 50 ml of distilled water with a solid/liquid ratio of 1:10 (w/w) after twelve hours equilibrate solution. Before each measurement, the pH meter was calibrated by standard buffer solution at controlled room temperature by using an effective fan system to maintain the temperature (Joshi et al., 2023).

3.3.3. Bulk density determination

The raw and activated bentonite clay was put into 100 ml of a graduated cylinder of known weight and avoided compression. The cylinder was tapped vigorously on the horizontal surface to constant clay volume. The volume of the packed clay was taken and apparent bulk density (AB) was calculated using the equation (5) (Leena et al., 2017).

$$AB = \frac{\text{Wa} - \text{Wb}}{\text{V}} \quad \text{Eq(5)}$$

Where AB is apparent bulk density (gm/cm^3)

Wa: weight of the cylinder plus clay;

Wb: weight of the empty cylinder; V: total weight of clay used after compression

3.3.4. Apparent Density Determination (ASTM D 1895 – 96)

The mass of the empty pycnometer was measured (MEP). Then approximately full of the pycnometer was filled with the raw and activated bentonite sample using funnel. After all the sample was passed through the funnel, the excess on the top of the cup was immediately scraped off with a straightedge without shaking the cup. Then the weight was measured and recorded (MSP). Since the pycnometer has definite volume the apparent density was calculated as follows equation 6 (Leena et al., 2017).

$$\text{PA} = \frac{\text{MSP} - \text{MEP}}{\text{VP}} \quad (\text{Eq. 6})$$

Where PA = Apparent density of raw bentonite, g/ml

MSP = mass of sample and pycnometer, g,

MEP = mass of empty pycnometer, g, and

VP = volume of pycnometer, ml.

3.3.5. Swell Index determination (ASTM D5890-95)

Powdered raw bentonite was tested after drying to constant weight at 105 °C and milled by laboratory milling apparatus to pass through a 45 μm test sieve. 2g of dried and finely grinded raw and activated samples were weighed. 90mL of distilled water was added to the clean 100mL graduated cylinder. The material was added approximately at a speed of 0.1 g/5 min. These steps were followed until the entire 2g sample had been added to the cylinder. After the final addition of the clay distilled water was added until it reached 100 ml. The sample is then covered and protected from disturbances for a period of 24 hrs, at which time the level of the settled and swollen clay is recorded and the free swelling index of bentonite clay was

calculated by using the equation (7) and the free swelling index was reported as the volume of swelled material (ml/2g) (Kiviranta et al., 2011, Leena et al., 2017).

$$\text{Free swelling index} = \frac{V - VO}{VO} \quad \text{(Eq. 7)}$$

Where V = volume of swelled and VO = the volume of dry bentonite samples

3.4. Structural and surface characterization of raw and activated bentonite

In this study the effect of the activation on the surface properties of the adsorbent was determined using different characterization tools such as X-ray diffraction (XDR), Fourier transform infrared spectroscopy (FTIR), X-ray fluorescence (XRF), TGA-DTA and scanning electron microscopy (SEM) and Point of zero charge (pHpzc) analysis. Detailed descriptions of these tools were discussed below.

3.4.1. X-ray fluorescence analysis (XRF)

The chemical compositions of the raw and activated bentonite samples were carried out using X-Ray fluorescence analysis (XRF Thermo Scientific) in the Chemical and Construction inputs development center laboratory.

3.4.2. Fourier infrared transforms (FITR) spectroscopy Analysis

The FT-IR technique was used to obtain functional groups on the surface of the raw and activated bentonite. The FT-IR spectroscopy (model 65 FT-IR PerkinElmer) recorded the spectra in the wavelength range of 400-4000 cm-1 using the potassium bromide (KBr) pellet method. For FT-IR characterization, 1 mg of the raw and sodium by carbonate activated bentonite sample and 100 mg of KBr were mixed with mortar and pestle. The small amount of fine powder from the mixture was pressed under 15 kpa pressure into a Pellet using a mechanical presser. Finally, the pellet was analyzed using a FTIR spectrometer to obtain the Infrared spectra from the pellet. The FTIR analysis was carried out in Addis Ababa University College of Natural and Computational Science, Department of Chemistry (Abdullahi et al., 2017,Pluangklang et al., 2021,Wasse Bekele et al., 2014).

3.4.3. X-ray diffraction (XDR)

The XRD is used to determine the crystalline or amorphous nature of the raw and activated bentonite. XRD patterns were determined using an X-ray diffractometer (XRD-7000) in

Adama Science and Technology University, at the Department of Applied Chemistry to study the amorphous or crystalline nature of the adsorbent materials. Appropriate sample amounts of the raw and activated bentonite were taken and then transferred to a rotating sample holder for XRD characterizations. Then the samples were analyzed by using an X-ray diffractometer with Cu-Kα radiation source at wavelength of K1 = 1.54060 Å and tube operating voltage of 40 kV and current 30 mA. The X-ray diffractograms were obtained for the 2θ angles scan range from 2˚ to 85˚ with scans step 0.02˚. All the experiments were done at room temperature, with a scans speed of 3˚/ min, using scintillation detector and continuous scan measurement mode with zero background sample holder

3.4.4. Differential thermal gravimetry (DTG) analysis

TGA coupled with DTA by a (Shimadzu co., DTG-60H, South Korea Japan) analytical instrument, was used to determine the thermal stability and percentage weight loss of the raw and activated bentonite, a function of temperature under a constant rate of heating. Thermogravimetric analysis was undertaken to investigate the effect of the activation of bentonite with sodium bicarbonate at temperature between 50 °C and 800 °C, with a heating rate of 15 °C/min which corresponds to the release of physically adsorbed water and the dehydration process. The total mass losses of raw and activated bentonite samples at temperatures ranging from 50 to 800 °C furthermore, to check if the TGA result is in agreement with the FTIR and XRD studies, TGA coupled with DTA by a (Shimadzu co., DTG-60H, South Korea Japan) analytical instrument, was used to determine the thermal stability and percentage weight loss of the raw and activated bentonite as a function of temperature under a constant rate of heating. An oven-dried adsorbent samples was heated from room temperature to 800°C in a Platinum/alumina cup with a heating rate of 15 °C/min, and an empty Platinum/alumina cup as control. 800°C was taken as the final temperature, because activated bentonite at this temperature is mostly stable implying no more degradation to take place (Wang et al., 2017).

3.4.5. Scanning electron microscopy (SEM)

The surface morphology of both raw and activated bentonite were examined using (JCM-6000PLUS BenchTop SEM, JEOL, Japan) using a high-energy electron, and the out coming electrons are analyzed by applying a 10 kV electron acceleration voltage in Adama Science

and Technology University, at the Department of Applied Biology. For SEM characterization, 30 mg sample were taken from each previously prepared samples and characterized by using SEM were the resulting images provides information about the surface features and texture, shape, size, and arrangement of the particles on the sample's surface a JSM-IT300 (LA) SEM at accelerating voltage of 20 kV, beam size 3.0, working distance 12.1 and magnification of 2500. Microscope images were taken to compare surface properties of raw and activated bentonite samples.

3.4.6. PH Point of zero charge (pHpzc) analysis

The value of the point of zero charge (pH pzc) of raw and activated bentonite was determined by using the solid addition method. 40 ml of 0.1 M NaCl solution were transferred to a series of 250 ml stoppered conical flasks. The different initial (pH_i) value of the 0.01 M NaCl was adjusted at pH (2-12) using 0.5 M HCl or 0.5 M NaOH were measured using a pH meter. The total volume of the solution in each flask was adjusted to exactly 50 cm^3 by adding NaCl solution of the corresponding concentration. The values of the solutions were adjusted between 2 and 12 by adding either 0.1 M HCl or NaOH and were measured using a pH meter. The pH of the 0.01 M NaCl was adjusted at different initial pH (2-12) using 0.5 M HCl or 0.5 M NaOH. The pH_i of the solution was then accurately recorded. 0.5 g of raw and activated bentonite was added to each flask, and the flask was securely capped immediately. The suspensions were then kept shaking for 0.5hr and allowed to equilibrate for 24 hr. The final pH values of the supernatant liquids were recorded. The differences between final and initial pH values (ΔpH) were calculated and plotted against the initial pH values. Therefore, the initial pH at which ΔpH is zero or the final pH was measured and plotted against the initial pH and the pH at which the curve crosses the pH initial equal to P^H final line was taken as the pHpzc (Obiageli et al., 2017, Unnithan et al., 2017).

3.5. Analytical method for chlorpyrifos identification and quantification on HPLC

After centrifuge was completed the supernatant was filtered using acridisk microfilter membrane (0.45 µm) of pore size syringe filter head prior to use and transferred into vials for chlorpyrifos identification and quantification on a high performance liquid chromatography equipped with a variable wavelength UV-vis diode array detector (Perkin Elmer 200 series) , series autosampler injector , quaternary pump, 900 series network linker, total chrome

software, vacuum degasser, solution filtration system, a C18- Reverse phase zorbax Ods, analytical column (250x4.6mm i.d., 3 µm) was used and maintained at room temperature 25 ^{0}C in a column oven. The mobile-phase reservoirs contained an 82/17.5/0.5 v/v % mixture of acetonitrile (A), water (B) and acetic acid (C) with a flow rate of 0.7 mL min−1 and isocratic elution was performed. The volume of the injection was 20 µL; the wavelength used for detection of chlorpyrifos was 290 nm with average retention time 5.85 min. The identification of the chlorpyrifos was performed by comparing peak retention times in samples to those of peaks in the pure analytical standard. Quantification was performed by collaboratively tested and validated methods approved by the Collaborative International Pesticides Analytical Council (CIPAC) or the Association of Official Analytical Chemists (AOAC International). CIPAC/AOAC methods of analysis for pesticide have been validated collaboratively for the quantitative determination of individual active ingredients (FAO/IAEA Division of Nuclear Techniques et al., 2009). The instrument's limit of detection (LOD) and limit of quantification (LOQ) were 0.00001 and 0.000015 mg/L. Method considered accurate and precise when the percentage of recoveries range between 70 -120 % and calculate as equation 8 (Fosu-Mensah et al., 2016) and when relative standard deviations, (RSD) of retention time and peak area are less than or equal to 2% and 5% for respectively for determined spike levels active substance (Köck-Schulmeyer et al., 2013). The percentage recoveries (Q) for the method were calculated using the following equation 8.

$$\mathrm{Q}\% = \frac{CE}{C\mathrm{M}} \times 100 \quad \text{..... (Eq. 8)}$$

Where CE is experimental concentrations of chlorpyrifos from calibration curve and CM is the spiked concentration of chlorpyrifos (Majumder, 2022, Hossain et al., 2015) and chlorpyrifos active ingredient content was calculated by using the following equation.

$$\text{Chlorpyrifos content (\% by mass)} = \frac{\mathrm{R2} \times \mathrm{W1} \times \mathrm{P}}{\mathrm{R1} \times \mathrm{W2}} \quad \text{.....(Eq. 9)}$$

Where: R2 is the response for the sample solution (R2 = area of sample peak), W1 is the weight of the chlorpyrifos standard, P is the purity of the chlorpyrifos standard, R1 is the response factor for the standard solution (R1= area of standard solution), and W is the weight of the sample .

3.6. Calibration curve of chlorpyrifos

The concentration of Chlorpyrifos lower than value determined in adsorption experiment the concentration of 5 levels in 100 ml volumetric flask mg/L) was measured on the using reverse phase HPLC system using acetonitrile as solvent. The Calibration curves for (0.015, 0.02, 0.025, 0.03, and 0.04 ml/L) chlorpyrifos in acetonitrile HPLC grade as solvent were figured by the peak area vs. initial concentration as indicated in the figure.11 (Abdelbagi et al., 2018).

3.7. Chlorpyrifos batch adsorption studies label

3.7.1. Preliminarily adsorption test for the selection of activated bentonite

Prior to batch adsorption experiments started, all adsorbents were dried overnight at 105 ^{o}C for 24 hr. The preliminarily adsorption test experiment was conducted to select the best adsorbent material among the six different prepared adsorbent including raw purified bentonite that labeled as RB and sodium bicarbonate activated (AB_2, AB_3, AB_4, AB_5, and AB_6). As indicated in (Appendix 1) the pre-test batch adsorption experiments were performed at pH 5, with 20 mg/15ml adsorbent dose, contact time of 60 minutes and initial concentration of chlorpyrifos 100 mg/L with shaking speed of 250 rpm at room temperature (Pluangklang et al., 2021). The adsorbent homogenized using an ultrasonic bath, ultrasonic vibration to disperse the dry clay particle aggregates in suspensions shaken at 30^{o}C which was then kept in a ultrasonic bath at 30 ^{o}C for 15 minute (Pluangklang et al., 2021). Subsequently, the suspensions were centrifuged at 3000 rpm for 15 min to separate the filtrate from the solid phase. After centrifugation, supernatant aliquots were filtered using acridisk microfilter membrane (0.45 µm) of pore size syringe filter head prior to pourig into vial for analysis by high-performance liquid chromatography (HPLC). The remaining residual pesticide concentration of chlorpyrifos, infiltrates/supernatants were analyzed by reverse phase HPLC which was equipped by a UV–Vis detector. All experiments were repeated three times, and additional analysis was performed when the difference between the two measurements was greater than 2% and 5% for retention and peak area present. The adsorption capacity of chlorpyrifos removed by the adsorbent was calculated as the adsorption capacity (milligram of chlorpyrifos adsorbed per gram of adsorbent (q_e)) and the percent adsorption/ removal efficiency (% R) by using equations 10 and 11 respectively (Farghali et al., 2020).

$$qe = \frac{co - ct}{w} \times v \ldots\ldots\ldots\ldots\ldots\ldots\ldots\ldots\ldots\ldots\ldots\ldots\ldots\ldots\ldots\ldots\ldots\ldots\ldots\ldots\ldots\ldots\ldots (Eq. 10)$$

$$\%R = \frac{CO - Ct}{CO} \times 100 \ldots\ldots\ldots\ldots\ldots\ldots\ldots\ldots\ldots\ldots\ldots\ldots\ldots\ldots\ldots\ldots\ldots\ldots\ldots.. (Eq. 11)$$

Where, qe is the chlorpyrifos quantity adsorbed at equilibrium (mg/g), Co is initial concentration of chlorpyrifos (mg/L), and Ct is the equilibrium chlorpyrifos concentration in solution after adsorption, w is adsorbent mass in gram and V is volume of chlorpyrifos solution (L).Based on preliminary adsorption capacity test the one activated with 5% sodium bicarbonate was found high adsorption capacity as indicated in (Appendix 1) and which was needed for further optimization by contact time, adsorbent dosage, pH value and initial chlorpyrifos pesticide concentration variables.

3.7.2. Optimization study of chlorpyrifos adsorption by activated bentonite

3.7.2.1. Effect of pH

To measure the effect of pH on the adsorption of chlorpyrifos by activated bentonite in the aqueous phase was investigated over the pH range of 2, 4, 6, 8, 10 and 12. Pesticide solutions were prepared by dissolving the samples in distilled water. The adsorbents were exposed to the pesticide solution at a solid/liquid ratio of 20mg/15ml with chlorpyrifos pesticide concentration 100 mg/L and 60 minute constant contact at 250 rpm in a volumetric flask with 50 ml which prepared by using stock solution. The solution pH was adjusted by adding 0.01M of HCl or NaOH solution, as appropriate. The pH was increased to approximately 11 with 0.01M NaOH before commencing the yield stress measurements. Solution of 0.01 M HCl was added drop wise to decrease the pH in a stepwise manner. The effect of pH on chlorpyrifos removal by the activated bentonite is graphically represented in Figure 7.

3.7.2. 2.The effect of contact time

The effect of conditioning time on the adsorption of chlorpyrifos, by the activated clay was investigated. 20mg bentonite clay is placed in flasks containing 15 ml of 100 mg/L aqueous solution of chlorpyrifos in a volumetric flask with 50 ml at optimum pH 6 which is prepared from stock solution. The contents of the flasks were equilibrated on the shaker at 250 rpm and 303 K. 5 ml of the solution (free from adsorbent particles obtained by filtration) were taken at 10minute time intervals and the residual concentration of chlorpyrifos was determined in

mg/g (from 10 min to 60 min) at each time interval (Amrety et al., 2018,Debebe et al., 2023,Senthilkumaar et al., 2010).

3.7.2.3. The effect of adsorbent dose

The amount of clay adsorbent was being varied from (10, 20, 30, 40, 50, and 60 mg) in 15ml pesticide solution with a constant initial chlorpyrifos concentration of 100 mg/L that was prepared from stock solution by using serial dilution system. Taking 100 ml into 1000 ml volumetric flask and the mixture was shaken using Thermostat shaker at 250 rpm and 303 K and kept agitation time 40 minute and pH 6 ±0.1 constant. The mixture is filtered and centrifuged. The uptake of chlorpyrifos is calculated by determining the residual concentration of chlorpyrifos in the supernatant according to the above method (Pluangklang et al., 2021).

3.7.2. 4. The effect of initial concentration

A constant clay amount of 30 mg was placed in a series of flasks containing 15 ml of pesticides solutions with different initial concentrations which was prepared from stock solution to (1, 50, 100,150, 200, and 250 mg/L) of chlorpyrifos by serial dilution. The contents of the flasks have been shaken at 250 rpm and 303 K for 40min at pH 6. After equilibrium, the residual concentration of chlorpyrifos was estimated and then the adsorbed amount was calculated. Figure 10 shows the chlorpyrifos adsorption capacity and the percentage of chlorpyrifos removal at various chlorpyrifos initial concentrations (Suciu et al., 2009, Amrety et al., 2018,Senthilkumaar et al., 2010).

3.8. Sample cleaning and extraction procedure for real sample analysis

The low density-based dispersive liquid-liquid microextraction (LD-DLLME) method was used for extraction of the target pesticide residues from wastewater real samples. Accordingly, a 15 mL water sample was taken into a 50 mL test tube and then, a mixture of 300 µL N-hexane and 1500 µL acetonitrile as extraction and disperser solvents respectively were rapidly injected using a 20 µL GC micro syringe. Subsequently, after the addition of 0.5 g NaCl, the content was shaken by hand until the salt was completely dissolved. Then the content was centrifuged for 15 min at 3000 rpm to facilitate the phase separation. A 50 µL of the floating organic phase was carefully withdrawn via a syringe and then transferred into

vials. Finally, 1 µL of the extract was injected into the high performance liquid chromatography (HPLC) system (Wang et al., 2017).

3. 9. Data analysis and interpretation

All data generated from the previously performed experiments were analyzed using the OriginPro 2021 and presented using tables and graphs.

3.10. Data quality control

Since data quality is essential for the validity of the adsorption experiment, quality control and quality assurance procedures were used to ensure the validity of the results. The equipments used for every single analysis were cleaned before using for analysis and all equipments were labeled to be used only for the research part separately. For this reason all glasswares equipment used were washed properly using detergent and distilled; rinsed with acetone to remove any non polar organic compound contaminants before dried into the oven. After adsorbents preparation, the adsorbents were put in desiccators to be free from any contamination for further analysis. To assist in maintaining the natural chemistry of the sample refrigeration and protecting from light was performed. The quantitative determination of chlorpyrifos pesticide residue in water was done on the basis of the external standard method. Identification of the pesticides was undertaken by running specific concentrations for each pesticide and by looking at the retention time. Calibration curves were plotted by taking concentration against the peak area each individual chlorpyrifos pesticides and the linearity of the calibration curve was validated using a correlation coefficient (R^2) were greater than 0.9712, over this covered range of initial chlorpyrifos concentration (Jemal et al., 2023).

3.11. Adsorption Equilibrium Isotherm Models

The adsorption isotherm depicts the interaction between the adsorbent and the adsorbate at constant room temperature under equilibrium conditions and also represents the effect of initial adsorbate concentration as a function of adsorbent dosage. Additionally, they provide information about the mechanisms of adsorption, adsorption capacity and surface properties. Basically the models employed are Langmuir, and Freundlich isotherm models (Baharum et al., 2020, Suciu et al., 2009).

The Langmuir isotherm assumes homogenous monolayer adsorption on the surface of adsorbent containing a finite number of binding sites, with uniform energies of sorption and no transmigration of sorbate in the plane of the surface. The linear Langmuir equation can be expressed as set out in Equation 12.

$$\frac{Ce}{qe} = \frac{1}{qmKL} + \frac{Ce}{qm} \quad \text{(Eq. 12)}$$

Where qe is the amount of chlorpyrifos adsorbed per unit weight of activated bentonite adsorbent (mg/g), Ce the equilibrium concentration of chlorpyrifos in the bulk solution (mg/L), qm is the monolayer adsorption capacity (mg/g) and KL is about the maximum monolayer saturation capacity or Langmuir equilibrium constant that obtained from the theoretical Langmuir model related to the energy of adsorption (L/g). KL is the reciprocal value of the concentration at which the adsorbent is half saturated. The essential characteristics of the Langmuir equation can be expressed in terms of a dimensionless separation factor RL. It was then calculated as stated in equation 13 that follows.

$$RL = \frac{1}{1 + bco} \quad \text{(Eq. 13)}$$

Where, Co is the initial chlorpyrifos concentration (mg/L) and b, Langmuir constant (Senthilkumaar et al., 2010).

The Freundlich isotherm assumes that the ratio of the amount of chlorpyrifos adsorbed onto a given mass of activated bentonite adsorbent to the concentration of the chlorpyrifos in the solution varies with concentration. The equation for Freundlich isotherm model can be described as Equation.14

$$\log q_e = \frac{1}{n}\log C_e + \text{Log}K_F \quad \text{(Eq. 14)}$$

Where, K_F the constant indicative of the relative adsorption capacity of the adsorbent (mg/g) and 1/n is related to the energy of adsorption effectiveness of the activated bentonite adsorbent is the constant.

3.12. Kinetics of adsorption

Kinetics study helps to select optimum operating conditions for the full-scale batch process, which have been applicable to investigate the mechanism of adsorption and potential rate controlling steps. Kinetic parameters are significant for the prediction of adsorption rate, and give useful information for designing and modeling the adsorption processes

(Senthilkumaar et al., 2010). Several kinetic models such as the pseudo first and second-order equations, intra-particle diffusion and Elovich equations are used to interpret the time dependent experimental data and examine the controlling mechanism of adsorption process (Joshi et al., 2023, Pluangklang et al., 2021, Amrety et al., 2018, Beigi et al., 2023). Therefore, the kinetics of chlorpyrifos pesticides adsorption onto 5% sodium bicarbonate activated bentonite adsorbent was analyzed by using pseudo-first-order and pseudo second-order kinetic models.

3.12.1. Pseudo-first-order model

The pseudo-frst order kinetic model, popularly known as the Lagergren (Shattar et al., 2020) rate expression. To describe the kinetic process of liquid-solid phase adsorption, it generally described by the equation as:

$$\log(qe - qt) = logqe - \frac{k1}{2.303} \quad \text{.....(Eq. 15)}$$

Where qe and qt (mg/g) are the adsorption capacities at equilibrium and at a time t (min), respectively, K1 (min-1) is the pseudo first order rate constant for the kinetic model (Pluangklang et al., 2021).

3.12.2. Pseudo-second-order model

The pseudo-second-order model is based on the assumption that the rate-limiting step may be chemisorptions, which involves valence forces by electron sharing or electron exchange between the adsorbent and the adsorbate(Pluangklang et al., 2021). Pseudo-second order equation is probably the most widely used model for adsorption kinetics. Most of the time this equation is used when the first-order model fails and the equation for this model is written as:-

$$\frac{\mathrm{t}}{\mathrm{qt}} = \frac{1}{\mathrm{qe}}\mathrm{t} + \frac{1}{\mathrm{k2qe}^2} \quad \text{.....(Eq. 16)}$$

where qe(mg/g) is the adsorption capacities at equilibrium; K2(g/(mg min)) is the equilibrium rate constant of pseudo-second order adsorption(Joshi et al., 2023, Pluangklang et al., 2021).

4. RESULTS AND DISCUSSIONS

4.1. Characteristics of the raw and activated bentonite adsorbent

4.1.1. Physicochemical characteristics of the adsorbent

The physicochemical characteristics of the adsorbent were assessed using the methods and procedures mentioned in the methodology. The pH of natural calcium bentonite is alkaline in nature because of the exchangeable cations and presence of excess hydroxyl groups in the structure of montmorillonite. The result was complementary with other findings. Since calcium bentonite is none swelling types of bentonite and the swelling index is much smaller than sodium bentonite. The swelling index of Ca -bentonite varies in the range of 10 - 15 ml/2g while Na-bentonite is more than 25 ml/2g since it absorbs more water. After activation, the pH as well as point of zero charge increase since more OH was released on the surface of bentonite due to cation exchange and the pH becomes more alkaline. The point of zero charge of raw bentonite is larger than the activated bentonite one because it contains more hydroxyl groups. The Swell Index or Free Swell test is used to determine the general swelling characteristics and type of bentonite clay. The result obtained in this study table (3) (Anupam et al., 2022) demonstrated that after activation the bentonite was converted to sodium rich bentonite with an average swell index of 18.2 ml/2g from calcium rich bentonite with average swell index 13.3 ml/2g. The result was complementary with other findings.

Table 3: Proximate composition and some characteristics properties of raw and activated bentonite adsorbents.

Bentonite types	pH-values	Swell Index (ml/2 g)	Apparent Density(g/cm^3)	Bulk density (g/cm^3)	M.C (%)
Raw bentonite	8.2	13.3	1.808	1.174	7.04
Activated bentonite	9.5	18.2	0.7205	0.7542	4.13

Constant weight of samples was obtained after 4 hr and the moisture content of the raw bentonite used in this study was found to be 7.04% using three replications. This indicates that in addition to free water, the interlamellar space of the raw bentonite contains variable amounts of water molecules, which are electrostatically bound and form hydrates with the exchangeable cations. The apparent density of milled bentonite products varies depending on mill fineness, ranging from 0.7 to 0.9 g/cm^3. The bulk density of clay is one of its most

informative properties, the bulk density is inversely proportional to the adsorptive capacity and to the clay's filtration rate. Swell Index test is an index method that enables evolution of swelling properties of materials containing expansive clay minerals. Output of this method is also a rough estimate of the smectite content in the sample and used to identify the type of bentonite. The result for swelling index of the raw bentonite was obtained around 13.3 ml/2g and similar as Ca-bentonite (non-swelling type) the result was complementary with other findings (Leena et al., 2017)**.** Both apparent and bulk density decreased after activation indicate that the increase of the surface area of bentonite clay is due to large surface area low density **as** clay expands with hydration and shrinks with dehydration when moisture content is released from the bentonite surface and interlamellar space **.**

4.1.2. X-ray fluorescent (XRF) Analysis

The changes of the chemical composition of the clay prior to and after activation listed in Table 4 were determined by X-ray fluorescence analysis (XRF), and it was observed that SiO_2, Al_2O_3, MgO, CaO, & Fe_2O_3 were the main components and K_2O, TiO_2, SO_2 and P_2O_5 were present as minor metallic oxides (Table 4) for both raw and activated bentonite clay. Representing the largest compositions of 45.92, 16.22, 9.38, 8.37 & 6.03% for raw bentonite and 41.31, 12.39, 7.48, 7.803, & 5.793% for activated bentonite clay. The XRF results revealed that when comparing the SiO_2/Al_2O_3 ratios of raw and activated bentonite, it shows that activated, has a higher and Al_2O_3/SiO_2 ratio with 0.38 and 0.30 for raw and 5% sodium bicarbonate activated bentonite respectively it shows that raw, has a higher (Table 4). These ratios indicated that natural bentonite and activated clay contained the montmorillonite mineral (Maged et al., 2020). Table 4 shows the effect of 5% sodium bicarbonate activation has a significant change on chemical composition. The weight percentage of metal oxide of Mg^{2+}, K^{+}, Ca^{2+}, Fe^{3+}, and Al^{3+} decreases significantly and whilst P_2O_5 and Na_2O what was expected increased due cations exchange with Na^{+} after activation with 5% sodium bicarbonate (Maged et al., 2020). Similar results were recorded according to (Obiageli et al., 2017).

Table 4: Chemical composition for raw and activated bentonite sample (% by weight).

No	Compound	Bentonite Sample	
		Raw bentonite	Activated bentonite
1	Al_2O_3	16.22	12.39
2	Fe_2O_3	6.03	5.795
3	TiO_2	0.7946	0.7273
4	CaO	8.327	7.8032
5	Free /active CaO	1.2	0.59
5	K_2O	3.2267	2.44
6	MgO	9.38	7.48
7	P_2O_5	0.08	0.2202
8	SO_2	1.66	0.4586
9	SiO_2	45.92	41.31
10	Na_2O	-	2.107
11	Al_2O_3/SiO_2	0.38	0.30
12	L.O.I	12.32	12.07

4.1.3. FT-IR Spectrophotometric Analysis

The FT-IR spectra of the raw and activated bentonite with 5% sodium bicarbonate exhibits absorption bands at 3430 and 3440 cm^{-1}, respectively; this is assigned to the stretching and bending vibrations of the OH groups for the water molecules and adsorbed on the surface of both raw and activated bentonite coordinated to octahedral Al^{3+} cations with different type response towards of the magnitude of the adsorption as stated by (Obiageli et al., 2017) (Figure 8). Besides, the intensity of band at 1629 and 1627 cm−1in the spectra of both raw and the activated bentonite was attributed to Si-O stretching vibrations (in-plane) of the tetrahedral sheets, whereas; the bands at 526 and 468 cm^{-1} correspond to Si–O–Al (where Al octahedral cation) (Obiageli et al., 2017) and Si–O–Si bending vibrations respectively (Wasse Bekele et al., 2014). The Si–O bands are strongly evident in the silicate structure of the original clay and can be easily recognized in the infrared spectrum by very strong absorption bands in the 1100–1000 cm^{-1} region. The most intensive band at 1019 cm^{-1} is attributed to Si–O in–plane stretching of raw bentonite. Similar results were reported by (Obiageli et al., 2017, Wasse Bekele et al., 2014). The FT–IR spectra of the natural raw and 5% sodium bicarbonate activated clay samples reflect the structural modification which takes place due to 5% sodium bicarbonate activation. Changes in the tetrahedral

sheets are reflected in the position and shape of the Si–O stretching band (Pluangklang et al., 2021).There is a slight decrease in the tetrahedral Si–O band intensity at 1014 cm−1 for the activated samples. This result suggests the partial depletion of Al, Mg and Fe from the clay structure, in accordance with the changes in chemical composition (Pluangklang et al., 2021, Wasse Bekele et al., 2014). The intensity of the bands at 3435 and 1635 cm^{-1} for water of hydration and the hydroxyl stretching band at 3618 cm^{-1} also shows increase after 5% sodium bicarbonate activation. It is due to the ion exchange of octahedral cations, causing the loss of water and hydroxyl groups coordinated to them. In addition, the transformation of the tetrahedral sheet was found at 792 cm^{-1}. The 5% sodium bicarbonate activation leads to the formation of amorphous silica, indicated by the increased intensity of the peak, which may expose more adsorption sites (Pluangklang et al., 2021). Most band positions did not change following modification, suggesting that the basic bentonite structure did not collapse (Obiageli et al., 2017, Wasse Bekele et al., 2014).These spectra confirm that the activated bentonite samples are still characteristic of bentonite.

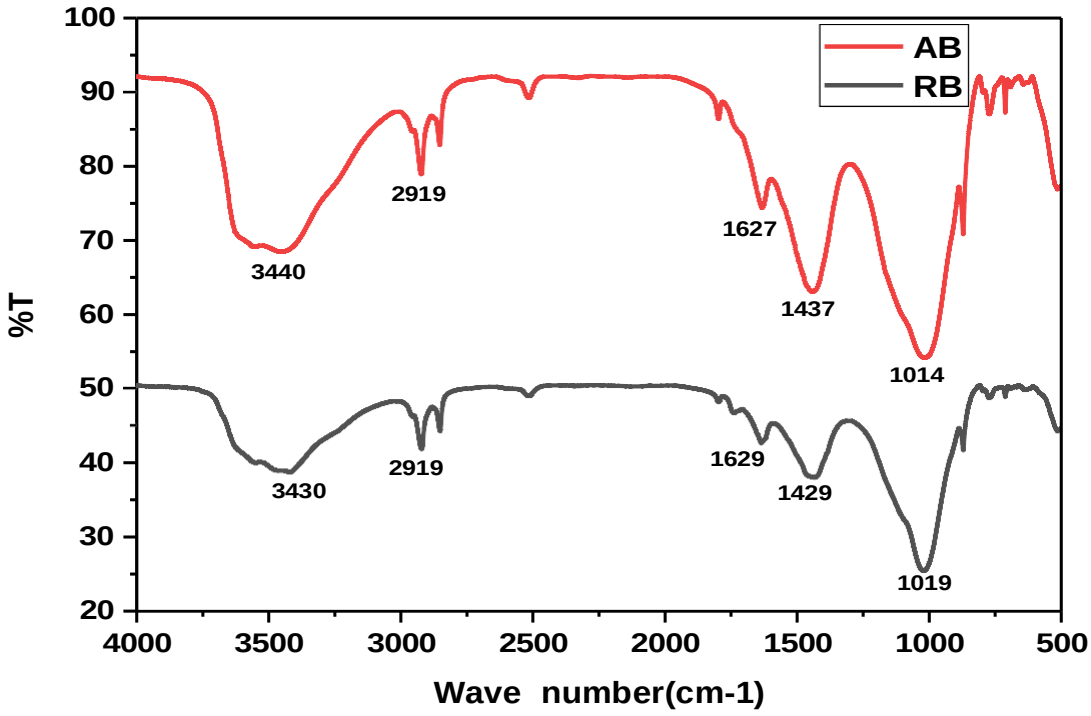

Figure 8:FTIR spectra for the raw and activated bentonite by sodium bicarbonate

4.1.4. Thermal stability analysis

Figure. 9 shows both thermogravimetric and differential thermal analysis (TGA-DTA) profiles of the raw and activated bentonite clay. Results of thermogravimetric thermal analysis (TGA) of raw and activated bentonite were contained two steps of weight loss. First stage of the decomposition occurred as the temperature changed from 52 – 107 ℃ which corresponded to an initial weight loss of around 2.265% or around 0.18 mg. This may be due to the moisture evaporation or low molecular weight volatile compounds. Second stage of the decomposition contributed to a major weight loss of about 0.9 mg as the temperature changed from 660 – 712 ℃. This weight loss is around 11.324% of the total initial weight. Above 600 ºC, the weight loss is traceable to the dehydration of some trapped water molecules in the interstices of the clay layers and due to dehydroxylation of the mineral, which is accompanied by a change in the crystal structure (Pluangklang & Rangsriwatananon, 2021).

The DTA of the clay was carried out to analyze the effect of heating on the surface and the structural properties of the clay. The dehydration stage corresponding to the removal of adsorbed and hydrated water loss from the pores of bentonite can be seen at 52 - 107 °C. This is the first endothermic peak. The removal of adsorbed and hydrated water provides additional adsorption sites, which results in surface area increase. The further heating is connected with a transition from dehydration to de-hydroxylation stage. The second endothermic peak appears at 528.3 ℃ there was a slight loss in mass due to partial loss of structural water (-OH) that indicates excess heat required to remove structural water from the bentonite sample and as revealed on different specific surface area as well as the cation exchange capacity of bentonite clay was increased without structural loss in the temperature range of 300 - 500 °C as shown in figure 9. And the endothermic maximums breaking between points at 660-712 ℃ were related to dehydroxylation. Heating beyond 800 ℃ are related to break of the crystal structure of 2:1 layers results in collapsing of the interlayer spaces, and consequently in clay structure rupture, which causes morphological changes and surface area decrease the same results revealed (Obiageli, 2017, Tadesse, 2022).

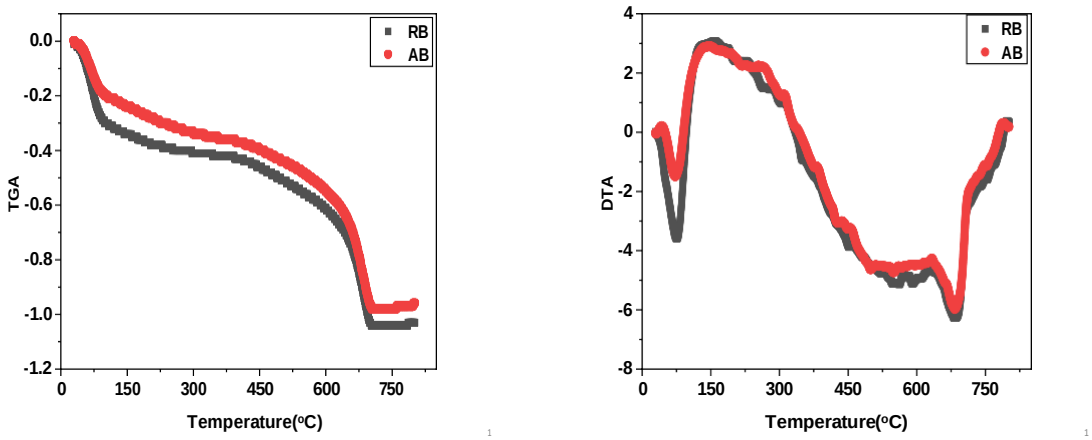

Figure 9: Differential thermal gravimetry (DTG) -analysis results of raw and activated bentonite.

4.1.5. XRD Analysis

The characterization of the clay samples by XRD aimed to verify the existence of associated minerals and clay minerals. The patterns showed the presence of diffraction peaks corresponding to angles (20, 26.67, 30 and 61.32), confirming the presence of montmorillonite in the samples. The data also showed the presence of impurities such as Muscovite (17.82), Cristobalite (22.12), Hematite (24.26 and 55.15), feldspar (28.01) and quartz (21.03 and 26.67) in bentonite clay evaluated. Similar results were reported. The differential thermal analysis curve confirms that the sample did not undergo phase changes and is thermally stable up to 500 ℃. Therefore, the crystallinity of bentonite was preserved and no significant difference on its crystalline structure except the quartz peak at 47 appeared and other quartz peaks enlargement were indicated after cation exchange due to partial conversion of Si^{+4} to SiO_2 and removal of impurities (Maged et al., 2020). Figure 10 shows the components of bentonite such as Montmorillonite (Mo), Muscovite (Mu), Quartz (Q), Cristobalite (C), Hematite (H), and feldspar (F).

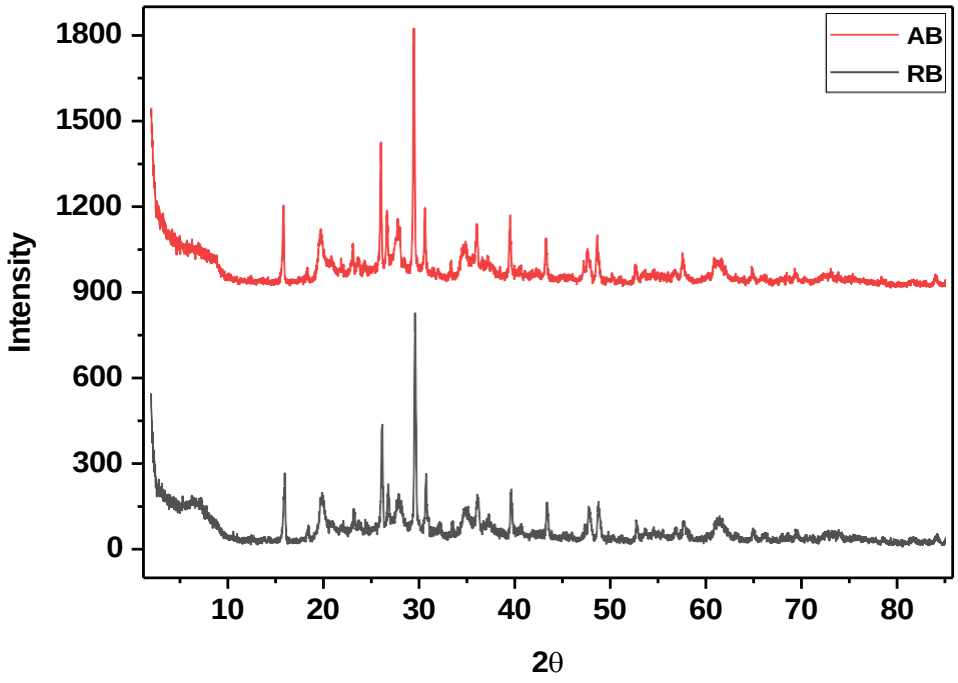

Figure 10: X-ray diffraction images of raw and activated bentonite.

4.1.6. Morphological features analysis

The SEM examination was carried out to assess the effect of the activation protocols on the surface morphology of the raw bentonite. The surface morphology of the raw and activated bentonite which are magnified 1500 times, as shown in figure 11. The morphology of raw bentonite, obviously the surface of this compound is different from activated bentonite images, indicating the 5% sodium bicarbonate activation makes the clay surface a little bit more porous and can create new pore. From the figure 11, the result shows activating the bentonite makes the clay surface a little bit more porous and can create new pore so that it will increase its surface area by cation exchange of divalent cation Ca^{+2}, Mg^{+2} with monovalent cation Na^{+1}

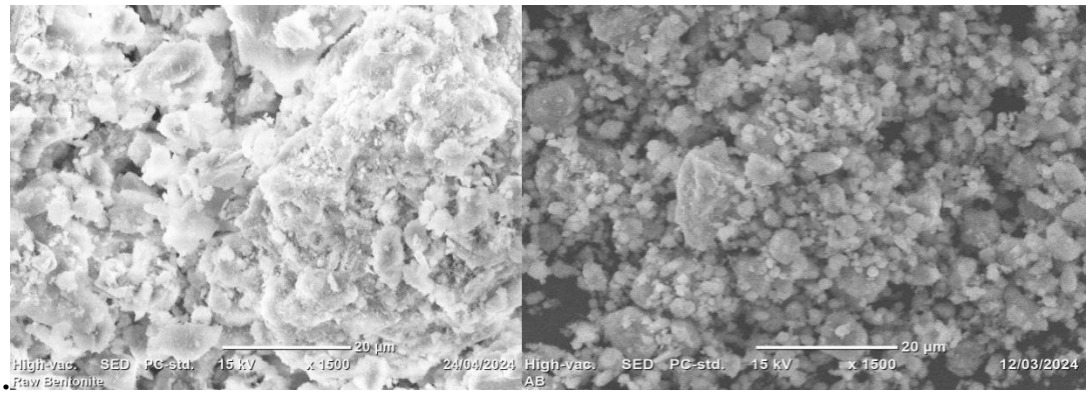

Figure 11: SEM micrographs for Raw Bentonite (RB) and Activated bentonite (AB).

4.1.7. PH Point of zero charge (pHpzc) analysis

The point of zero charge (pHpzc) of an adsorbent is the pH value at which the total number of positive and negative charges on its surface becomes zero. The pH at the point of adsorbent zero charge (pHpzc) was measured by using the pH drifts method (Unnithan et al., 2017, Obiageli et al., 2017). Figure 12 indicates that the pHpzc of adsorbent raw and activated bentonite were 8 and 9.1 respectively, where the ΔpH values were zero. It has been reported (Obiageli et al., 2017) that the pHpzc of an adsorbent decreases with increase of the alkaline groups on the surface. After activation, the pH as well as point of zero charge increase since more OH was released on the surface of bentonite due to cation exchange and the pH becomes more alkaline. The point of zero charge of activated bentonite is larger than the raw bentonite one because it contains more hydroxyl groups. The results obtained in this study lead to the conclusion that the 5% sodium bicarbonate activation of the raw bentonite adsorbent provides a negative (more alkaline) surface charge as the pHpzc value of the activated bentonite surface is found higher than that of the raw bentonite.

Table 5: Data of pHpzc of raw and activated bentonite by sodium bicarbonate.

S/NO	Initial Ph		Final pH	
	Raw	Activated	Raw	Activated
1	2.2	2.0	7.9	8.9
2	3.0	3.1	8.1	9.1
3	4.0	3.9	8.0	9.0
4	4.9	5.1	8.1	9.1
5	6.0	6.0	8.1	9.1
6	6.9	7.0	8.1	9.1
7	8.0	7.8	8.0	9.1
8	8.9	9.1	8.0	9.1
9	10.0	9.9	8.1	9.1
10	11.0	11.2	8.1	9.1
11	12.0	12.0	8.0	9.0

The relationship between the pHpzc value and the adsorption capacity indicates (Obiageli et al., 2017) that cations adsorption was expected to increase at pH value higher than that of the pHpzc, while anions adsorption was favorable at pH values lower than that of the pHpzc. Thus, the high uptake capacity was observed at pH 6 had been confirmed the nonionic property of chlorpyrifos changed into cationic at the lower pH value and the negatively charged bentonite surface has electrostatic attraction between surface of activated bentonite adsorbent and chlorpyrifos (Obiageli et al., 2017).

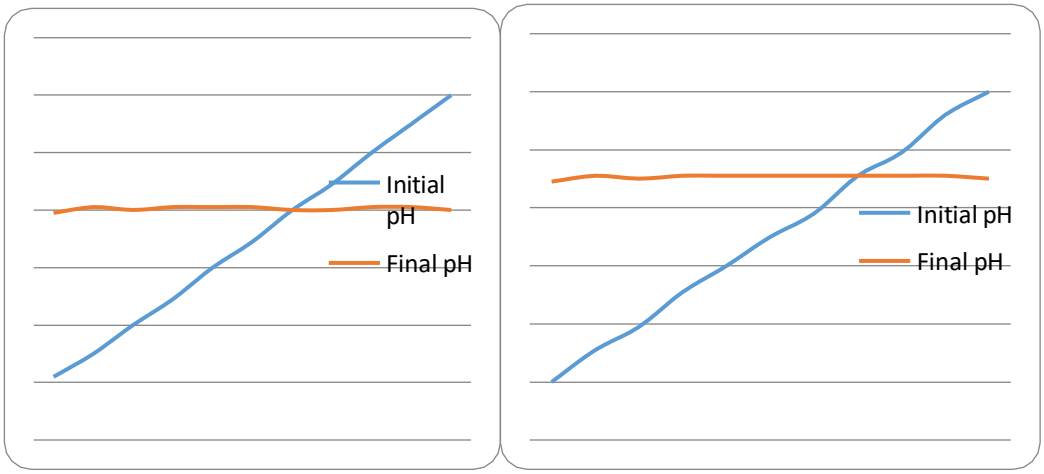

Figure 12: pH point of zero charge (pHpzc) of raw and activated bentonite from left to right.

4.2. Batch Adsorption Experiments

4.2.1. Chlorpyrifos Data

The accuracy of total analysis via HPLC was checked by running blanks and duplicate chlorpyrifos standard reference material. The chlorpyrifos sample solution was identified by a comparison of its relative retention time to the peaks from the calibration standards (Pluangklang et al., 2021). The analysis utilizes reversed-phase high-performance liquid chromatography (RP-HPLC) followed by UV-vis diode array detection. The precision was evaluated for the retention times and peak areas of the same sample, and the estimated values for relative standard deviation (RSD) was less than or equal 2% and 5% respectively, which indicated an excellent precision of the proposed method. Under the established conditions, the percentage of recovery of the analyte was between 70-120 %. This method was successfully applied for determination of chlorpyrifos pesticide in aqueous solution (Velkoska-Markovska et al., 2018).The instrumental limit of detection for chlorpyrifos analyte was 0.00001mg/L.

4.2. 2. Calibration Curve of Chlorpyrifos

The relationship between peak area and gradient concentration (0.015, 0.02, 0.025, 0.03, and 0.035 mg/L) of the 5 level chlorpyrifos calibration curve are shown in Figure (13). It is obvious that the peak area increased linearly as the concentration of chlorpyrifos increased in the solution. These findings indicate a linear relationship. Regression analysis showed a correlation coefficient (R^2) of 0.9712 for chlorpyrifos indicating a strong positive association. This linearity indicates the validity and the suitability of the used method and allows direct measurements of pesticides in the supernatants. Each time, solution concentrations were determined before running the experiment and measured multiple times 2–3 to reconfirm the concentrations. These values were quite satisfactory and meet the requirements of the Quality Control of Pesticide Products prepared by the Joint FAO/IAEA Division of Nuclear Techniques in Food and Agricultural indicated that the concentration curves were prepared using the same HPLC methods as the sample preparation except chlorpyrifos standard was directly suspended in acetonitrile instead of being diluted by water by serial dilution system. OriginPro 2021.lab.Software was used to determine the linear relationship for chlorpyrifos concentration (C) based on the area (A) under the HPLC curves shown in the Appendix-2. Based on the result the absolute difference between two single test results obtained with the

same method on identical test material under the same conditions the these recovery values show that the method used was reproducible (Fosu-Mensah et al., 2016, Leena et al., 2017).

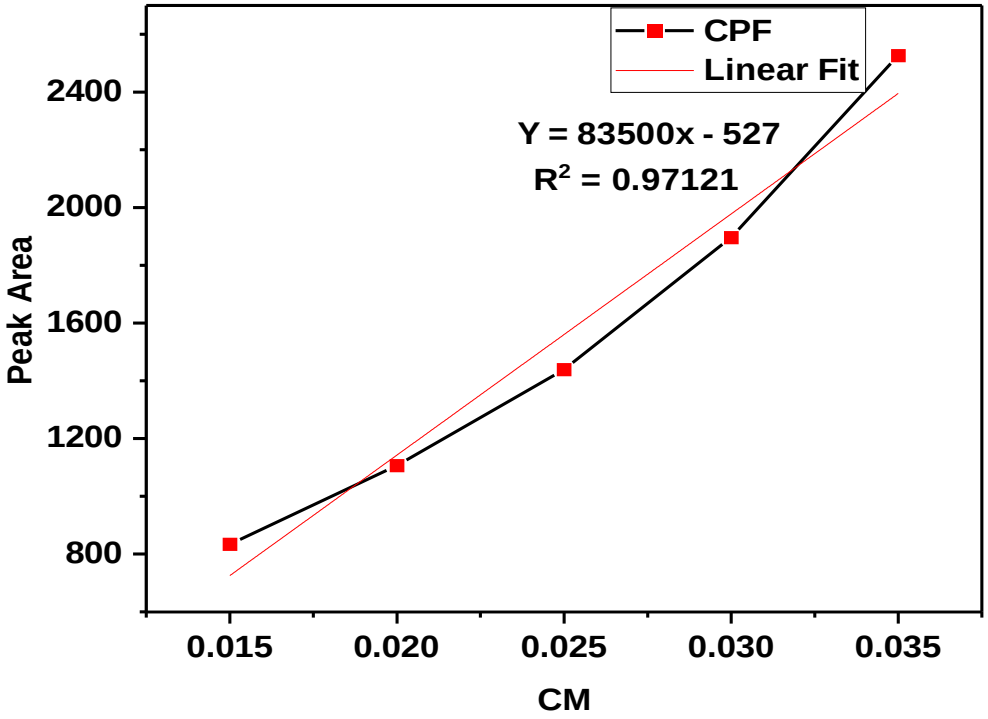

Figure 13: Calibration curve for chlorpyrifos analysis

4.3. Optimization study for removal of chlorpyrifos from aqueous solution

4.3.1. Effect of P^H

The impact of solution pH on CPF removal by activated bentonite adsorbent was investigated at over pH ranges of (2, 4, 6, 8, 10 and 12) at a chlorpyrifos concentration of 100 mg/L. According to the results shown in Figure 13, it is obvious that the adsorption of chlorpyrifos on to the activated bentonite adsorbent was strongly pH-dependent. The changes in pH of the solution affect the speciation of adsorbate species, adsorbent surface charge, and degree of pesticide ionization. According to (Pluangklang et al., 2021), the activated bentonite contains precipitated Al^{+3} and Fe^{+3} hydroxides with strong affinity for anionic species. Thus, electrostatic interactions are quite possible between various anions such as S, O, N and Cl of CPF and cations of Al, Fe, etc atoms of activated bentonite. At the acidic pH, the surface of AB was positively charged, and this suggested that the interaction between the adsorbent and chlorpyrifos at pH < 6 is governed by the electrostatic force between the positively charged AB and the electron rich regions such as S, O, N and Cl in the adsorbed molecules of

chlorpyrifos. Thus the higher removal percentages of chlorpyrifos at acidic pH range (2 to 6), resulted higher adsorption due high electrostatic attraction in between electron rich regions of chlorpyrifos species and positively charged surface of activated bentonite (Pluangklang et al., 2021, Shattar et al., 2020). Chlorpyrifos absorption improves gradually with increasing pH, and the highest percentage removal (R %) efficiency of chlorpyrifos 96.44% and 39.511 mg/g adsorption capacity were achieved at pH 6

Thus, the solution pH of 6 provides the minimum amount of cationic and anionic substances, diminishing their impact on the chlorpyrifos and activated bentonite active sites' interactions. In this regard, for the chlorpyrifos with a positively-charged structure, the driving forces for its adsorption on the 5% sodium bicarbonate activated bentonite with negative surface charge are the electrostatic attraction, which led to an enhanced adsorption capacity at solution pH 6. This result was consistent with (Beigi et al., 2023). The removal percentage increased by raising the pH level over 8 to 12 due to the stability of chlorpyrifos decreased as the pH increased. The

half-life of chlorpyrifos in distilled water at pH 4.7 , pH 6.9 , pH 8.1 and pH 10 was 63, 35,23,and 4.57 days at 25 ^{o} C respectively (Hui et al., 2010). Thus, the optimum pH of adsorbate occurred at pH 6 which is consistent with reported studies (Amrety et al., 2018, Jemal et al., 2023) and thus the result was found similar with (Beigi et al., 2023, Hui et al., 2010, Bokulić Petrić et al., 2023) the maximum removal percentage of chlorpyrifos at higher pH at more alkaline were due to alkaline hydrolysis reaction of chlorpyrifos pesticides.

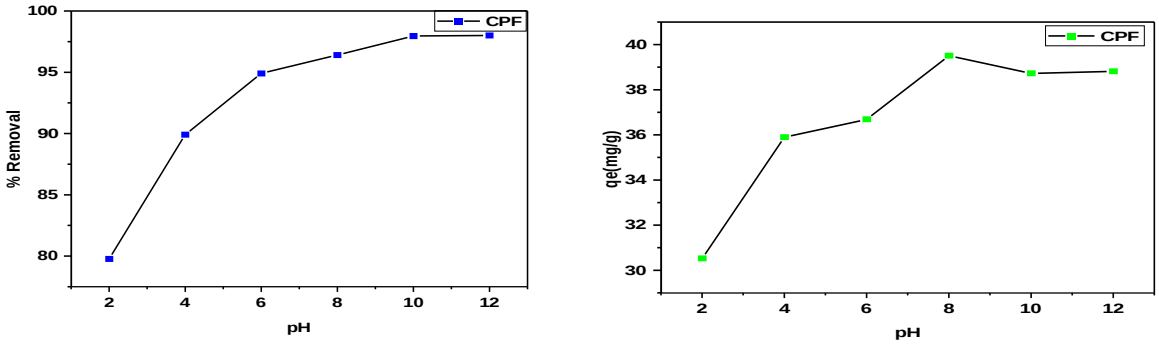

Figure 14: Variation in removal efficiency of chlorpyrifos with pH (Initial concentration = 100 mg/L, activated adsorbents dosage = 0.02 g, contact time = 60 min and at room temperature =25°C).

4.3.2. The effect of contact time

Contact time is an important parameter to determine the equilibrium time of the adsorption process. The effect of contact time conditioning on the activated bentonite adsorbent to adsorb chlorpyrifos was investigated. To determine equilibrium time, other parameters were kept constant with 0.02 g of adsorbent (activated bentonite clay) mixed with chlorpyrifos solutions (100 mg/L) of 15 ml volume and at pH 6. Experimental determination of chlorpyrifos was then done after the mixture was shaken at 25 °C and for the desired time. The experiment was done for contact time of 10, 20, 30, 40, 50 and 60 minutes. In this regard, the chlorpyrifos adsorption capacity demonstrates an increasing trend as the time progreses from 10 to 40 minutes of chlorpyrifos percentage removal from 81.89 to 95.97 % and however the adsorption capacity decreases slightly as the time progress from 50 to 60 minutes. However, the increase was not significant for longer contact time (Figure 15) thus shows, an optimum contact time for chlorpyrifos was ascertained as 40 min with 95.97% removal percentage with 37.11 mg/g adsorption capacity. This trend could be attributed to the fact that at the initial time between 10-30 minutes, there exist a number of vacant sites on the adsorbent but after 40 minutes these sites are occupied with the adsorbate molecules. And the contact time between 50 and 60 minutes, the repulsive force between solute molecules and bulk phase becomes significant and the vacant sites remain constant with time. This observation agrees with the literature reported by (Amrety et al., 2018, Debebe et al., 2023, Senthilkumaar et al., 2010).

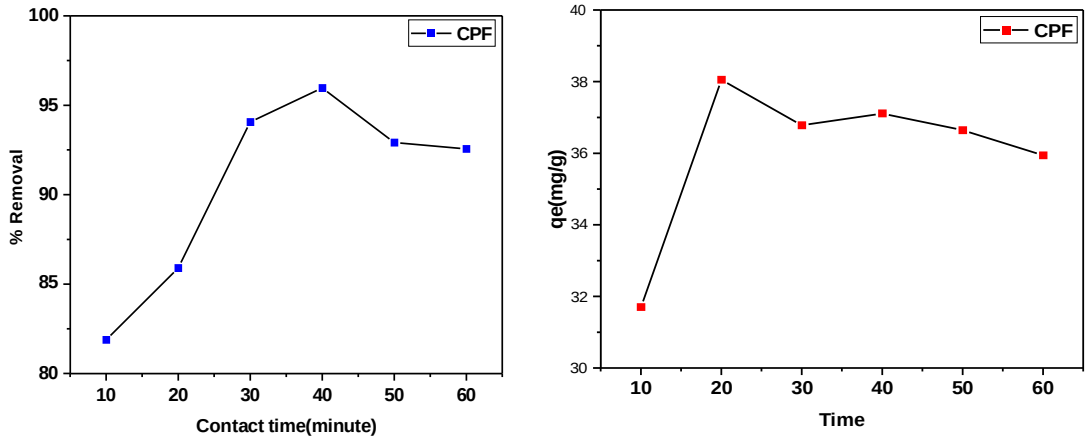

Figure 15: Variation in removal efficiency of chlorpyrifos with contact time (Initial concentration = 100 mgL^{-1}, activated adsorbents dosage = 0.02 g, pH 6 and at room temperature = 25 °C)

4.3.3. The effect of adsorbent dose

The relation between the activated bentonite adsorbent amount from 10 mg to 60 mg in 15 ml volume pesticide solution with a constant chlorpyrifos initial concentration (100 mg/L) and at optimum contact time 40 minute and pH 6 in 25 ml test tubes in related to adsorption capacity for CPF was investigated. The percent removal efficiency was plotted against AB dose to evaluate the impact of AB dose, which is shown in Figure16. A maximum removal of 98.24 percent of CPF insecticides was observed with the activated bentonite at a 2.67 g/L dose. Activated bentonite with an adsorption capacity of 0.67g/L exhibited the least. The removal percentage of AB increases as the dose increases because of many adsorption sites. However, chlorpyrifos uptake steadily decreases due to two factors: first, many adsorption sites are available for the same quantity of chlorpyrifos, and second, a high quantity of activated bentonite in a small amount accessible space clumps together, limiting the diffusion and adsorption path. Similar result reported by (Joshi et al., 2023, Baharum et al., 2020).

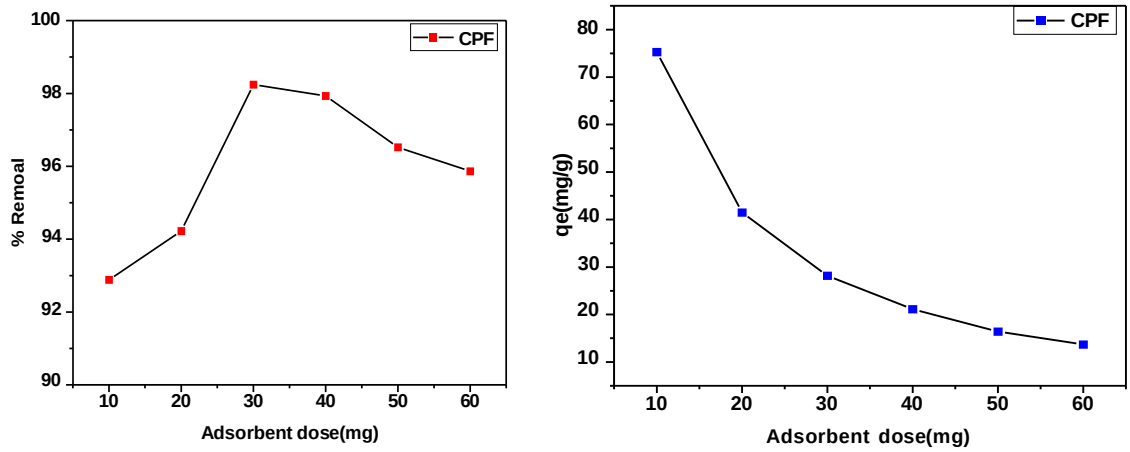

Figure 16: Variation in removal efficiency of chlorpyrifos with different activated adsorbents dosage (Initial concentration = 100 mg/L, contact time = 40 min, pH 6 and at room temperature = 25 °C)

4. 3.4. The effect of initial concentration

A constant clay amount of 30 mg is placed in a series of flasks containing 15ml of pesticides solutions with different initial concentrations of chlorpyrifos (1, 50, 100, 150, 200, and 250 mg/L). The contents of the flasks have been shaken at 250 rpm and 303 K for 40 min. After equilibrium, the residual concentration of chlorpyrifos was being estimated and then the

adsorbed amount was calculated. Figure 17 shows the chlorpyrifos adsorption capacity of 5% sodium bicarbonate activated bentonite and the percentage of chlorpyrifos removal at various chlorpyrifos initial concentrations (Suciu et al., 2009, Amrety et al., 2018, Senthilkumaar et al., 2010). The results show increases in the amount of sorbed CPF per unit mass with increase in CPF initial concentrations due to the escalation in the mass driving force that permits more CPF molecules to pass from the solution to the surface of the adsorbent (Hamadeen et al., 2021). The results indicated that the adsorption capacity increases with increasing the initial Chlorpyrifos concentration. These results are similar to experiments obtained by (Amrety et al., 2018). The increase in adsorption capacity with concentration is probably due to a high driving force for mass transfer. In fact, high concentration in solution implicates high molecules of chlorpyrifos fixed at the surface of the adsorbent (Amrety et al., 2018)

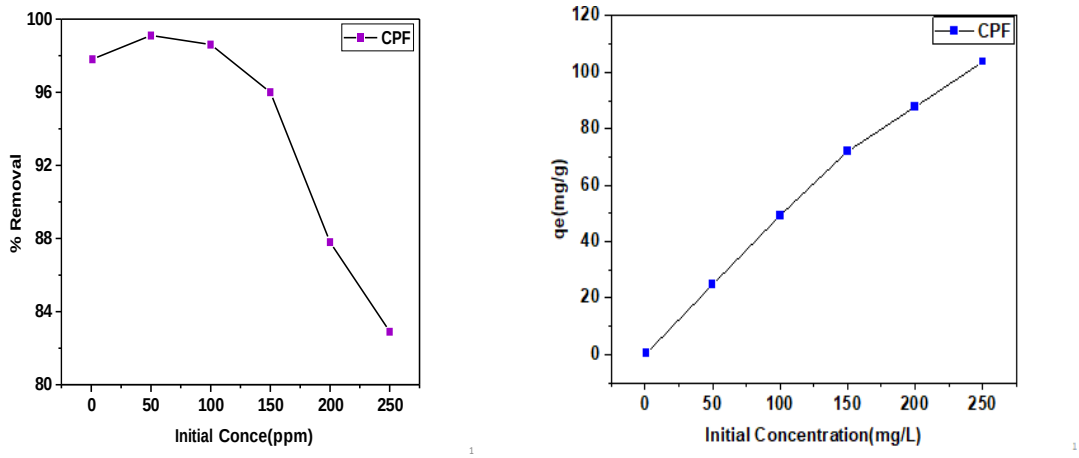

Figure 17: Variation in removal efficiency of chlorpyrifos with initial concentration of adsorbate (activated adsorbents dose = 0.03 g, contact time = 40 min, pH = 6 and at room temperature = 25 °C).

4.4. Adsorption equilibrium isotherm models

The adsorption equilibrium provides important physicochemical data for evaluating the applicability of the adsorption process as a unit operation. In this study, the equilibrium data were analyzed by using Langmuir and Freundlich isotherm models. These are generally related to the type of coverage, the possibility of interaction between the adsorbent

and adsorbate species, the heterogeneity and homogeneity of the adsorbent (Pluangklang et al., 2021). Adsorption isotherms for chlorpyrifos were acquired by batch equilibration using 30 mg of activated bentonite in 15 mL of aqueous pesticide solution at various concentrations (1 – 250 mg/L) at pH 6 ± 0.01. After equilibration (40min), solid and liquid phases were separated by centrifugation. Chlorpyrifos concentration was determined by HPLC which was equipped with a UV–Vis detector by measuring absorbance at 290 nm. Data obtained from the adsorption tests were used to calculate isotherm models that relate adsorbate per unit weight of adsorbent (qe) to the equilibrium adsorbate concentration in the bulk fluid phase (Ce). The adsorption isotherms relate the adsorbed amounts of chlorpyrifos pesticides were evaluated by applying the Langmuir and Freundlich models**.**

4.4.1. Langmuir adsorption isotherm model

From all isotherms commonly used for describing adsorption, the Langmuir adsorption isotherm model is the best known, and it has been successfully applied to various adsorption processes. The Langmuir isotherm is effective for adsorption of a solute from a liquid solution as monolayer adsorption on a surface containing a fixed number of identical sites. The experimental data were analyzed according to the linear form of the Langmuir isotherm as described in Equation 12. The linear plots of 1/qe versus 1/Ce suggest that Langmuir isotherms for the removal of CPF from aqueous solution by activated bentonite are applicable. Figure 18 showed the experimental results obtained from the Langmuir isotherm experiment. The experimental conditions of pH 6, adsorbent dosage of 0.03 g, agitation speed 250 rpm at room temperature being kept constant with various initial concentrations ranging from 1, 50,100, 150, 200 to 250 mg/L. The values of qm and KL of linear expression of Langmuir adsorption isotherm were calculated from the slopes and intercept of the linear plot of 1/qe versus 1/Ce shown in Figure 18. As presented in Table 6, the correlation coefficient value (R^2=0.9894) indicates that the Langmuir model adequately fits to describe the equilibrium adsorption of CPF pesticides onto activated bentonite adsorbent. The well – fitting of the Langmuir model also shows the presence of monolayer CPF coverage on the homogeneous active sites of activated bentonite adsorbent. The Langmuir model can also be used to determine the feasibility of CPF insecticides adsorption onto activated bentonite adsorbent based on the RL value which is dimensionless constant expressed in equation 13 (Pluangklang et al., 2021). The result obtained from the RL values illustrates the fit of

activated bentonite as an adsorbent in adsorption study in the Langmuir model. The value of RL = 1 shows a linear relationship between adsorbent and adsorbate whereas RL> 1 implies the unfavorable relationship while 0 < RL< 1 indicates the favorable isotherm and RL = 0 points out an irreversible relationship. The RL value for the activated bentonite adsorbent in this study is 0.011, implying favorable adsorption for CPF pesticides from aqueous solution (Senthilkumaar et al., 2010). The maximum chlorpyrifos adsorption capacity of the activated bentonite adsorbent determined from the Langmuir isotherm model was found to be 3.659 mg/g. The value of RL indicates the type of the isotherm to be unfavorable, linear or favorable. The obtained RL value was greater than 0 but less than 1(0.011), as shown in Table 6, indicating that the adsorption processes of CPF by activated bentonite by 5% sodium bicarbonate as adsorbent was favorable.

Table 6: Summary table for the line fit graph of Langmuir isotherm model

Pollutant	Co(mg/L)	Intercept	Slope	qm(mg/g)	KL	RL	R^2
CPF	52.45	0.1589	0.2733	3.659	1.720	0.011	0.9894

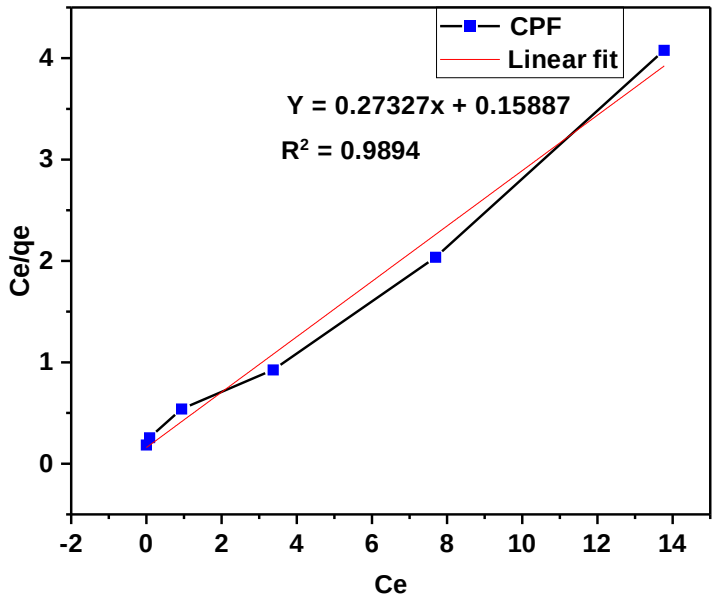

Figure 18: Langmuir adsorption isotherm model.

4.4.2. Freundlich adsorption isotherm model

The Freundlich isotherm model was the second model used to describe the adsorption data of chlorpyrifos pesticides in which the Freundlich constant KF (mg/g), and n is characteristic constants related to the relative adsorption capacity of the adsorbent and the intensity of adsorption, respectively. The KF and 1/n can be obtained from the intercept and slope of the linear plot of Logqe versus LogCe can be described as equation14. The Freundlich plots between Logqe versus LogCe for the adsorption of chlorpyrifos are shown in Figure 19.The applicability of the Freundlich adsorption isotherm was also analyzed, using the same set of experimental data as for the Langmuir model. The obtained n values from the Freundlich model lying between 1 and 10 (2.0045) indicates the favorability of the reaction. The slope (1/n) ranges between 0 and 1 and it is a measure of adsorption intensity or surface heterogeneity. It becomes more heterogeneous as its value gets closer to zero whereas a value below 1 implies the chemisorption process as the main adsorption mechanism and above 1 is indicative of cooperative adsorption. In this study, as confirmed on the Freundlich isotherm model, being the value of 1/n closer to one (0.50) shows the homogeneous nature of the activated bentonite adsorbent surface and the type of adsorption is a chemisorption process . Thus, From Table 6, The Langmuir isotherm exhibited a better mathematical fit to experimental data (R^2= 0.9894) than the Freundlich isotherm (R^2=0.9785), suggesting that the adsorption of the CPF insecticides onto activated bentonite adsorbent could be favorably described by the Langmuir model. These results indicated that the adsorption process of CPF on the surface of activated bentonite adsorbent was the monolayer adsorption. Similar results were obtained by different studies for activated bentonite adsorbents (Joshi et al., 2023, Pluangklang et al., 2021, Amrety et al., 2018).

Table 7: Result of the line fit graph of Freundlich isotherm model.

Pollutant	Co(mg/L)	Intercept	Slope	N	KF	R^2
CPF	52.45	-0.8703	0.4988	2.0045	0.1348	0.9785

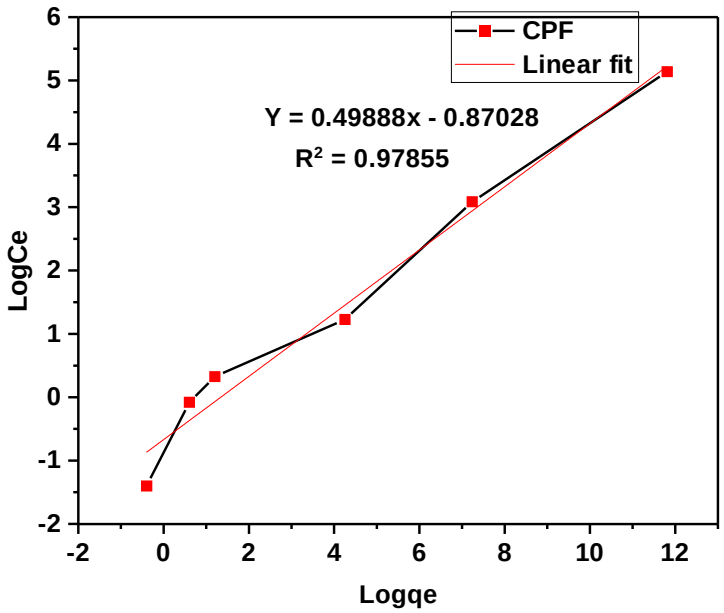

Figure 19: Freundlich adsorption isotherm model.

4.5. Kinetics study

The kinetics study was done using pH 6, initial chlorpyrifos concentration of 50 mg/L, adsorbent dosage 0.03 g, contact time ranging from 10 - 60 min and agitation speed 250 rpm at room temperature. By using the correlation coefficient significance, the conformity between experimental data and the model-predicted values were expressed.

4.5.1. Pseudo-first order kinetic model

To determine whether the adsorption process fits with the pseudo-first-order model or not, the experimental data using contact time ranging from 10 - 60 min and pH 6, initial chlorpyrifos concentrations 52.45 mg/L, adsorbent dosage of 0.03 g at room temperature, and 250 rpm agitation speed were introduced to Equation 15 (Figure 20). From the slopes and intercepts of pseudo-first order model [Log (qe-qt) versus t] (Figure 20), the first order rate constant, k1 and equilibrium adsorption density, qe were determined. The kinetic parameters obtained from the models are given in Table 8. The qe and correlation coefficient (R^2) values calculated using pseudo -first order model were found to be 19.49 mg/g and 0.9794 respectively. This indicates that there is great variation between calculated (19.49 mg/g) and

theoretical (37.11 mg/g) qe values. Thus the experimental data could not be well described by a pseudo-first order model.

Table 8: Results of line fit model of pseudo-first order kinetic.

Pollutant	Co(mg/L)	qe,exp(mg/g	qe,cal(mg/g)	K1	R^2	Slope	Intercept
CPF	52.45	37.11	19.49	0.1859	0.9794	-0.0807	1.2898

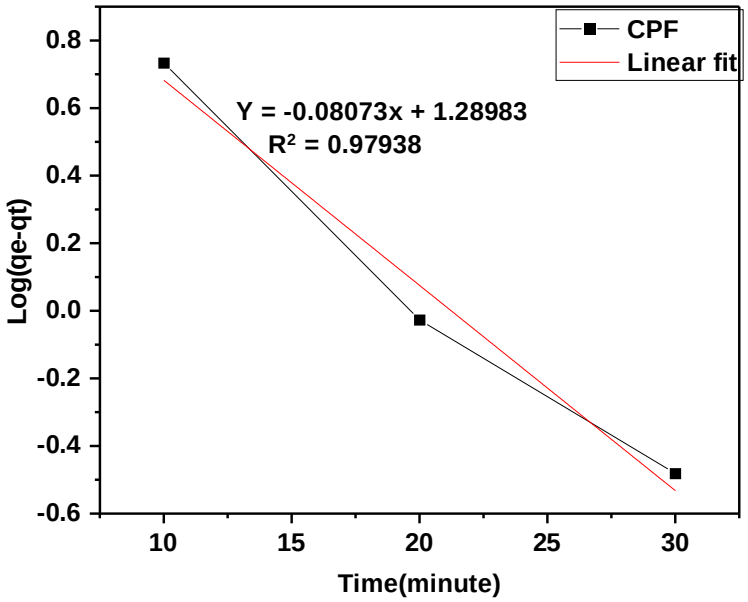

Figure 20:Pseudo-first order kinetic plot for the adsorption of CPF pesticides onto activated bentonite adsorbent.

4.5.2. Pseudo-second order kinetic model

In addition to the pseudo-first-order kinetics model, the linearized form of the kinetic rate expression for a pseudo-second-order model was applied to the experimental data. Calculated equilibrium adsorption capacity qe (cal), pseudo-second-order rate constant (K_2), and the correlation coefficient (R^2) were obtained from the model using Equation 16. The linear plots of t/qt against time are shown in Figure 21 for CPF pesticides adsorbed on activated bentonite adsorbent. From the slope and intercept of pseudo –second order model, t/qt versus t (Figure 21), the value of qe and K_2 were determined. The kinetic parameters obtained from the models are given in Table 9. Pseudo second-order reaction rate model which give a linear relationship adequately described the kinetics of adsorption of CPF with high correlation

coefficient (R^2= 0.9976) and its theoretical equilibrium adsorption capacities qe (exp) (37.11mg/g) fit well with the calculated qe (36.65 mg/g) data. Figure 21 and Table 9 showed the value of R^2 on pseudo-second-order for CPF pesticides is higher than on pseudo first-order kinetics and the calculated adsorption capacity qe (cal) was closer to the experimental adsorption capacity qe(exp), indicating that the pseudo -second-order kinetic model describes the adsorption process of CPF pesticides by activated bentonite adsorbent perfectly. This indicated that the pseudo-second-order model better represents the chlorpyrifos adsorption kinetics. A similar fit to this model has also been reported (Joshi et al., 2023, Beigi et al., 2023, Pluangklang et al., 2021).

Furthermore, the relatively high R^2 for the pseudo-second-order model (Table 9) indicates that the chlorpyrifos adsorption on the adsorbents was likely via the chemisorption process. This observation was in agreement with the findings of other studies on chlorpyrifos adsorption by clay of EL gash river (Amrety et al., 2018), pectin hydrogel@Fe_3O_4-bentonite (Beigi et al., 2023) and bentonite treated with heat and acid for adsorption atrazine, diuron paraquat and 2,4-D (2,4-dichlorophenoxy acetic acid) (Pluangklang et al., 2021).

Table 9: Results of line fit model of pseudo – second order kinetics.

Pollutant	Co(mg/L)	qe,exp(mg/g)	qe,cal(mg/g)	K_2	R^2	Slope	Intercept
CPF	52.45	37.11	36.65	0.0874	0.9976	0.0273	0.0085

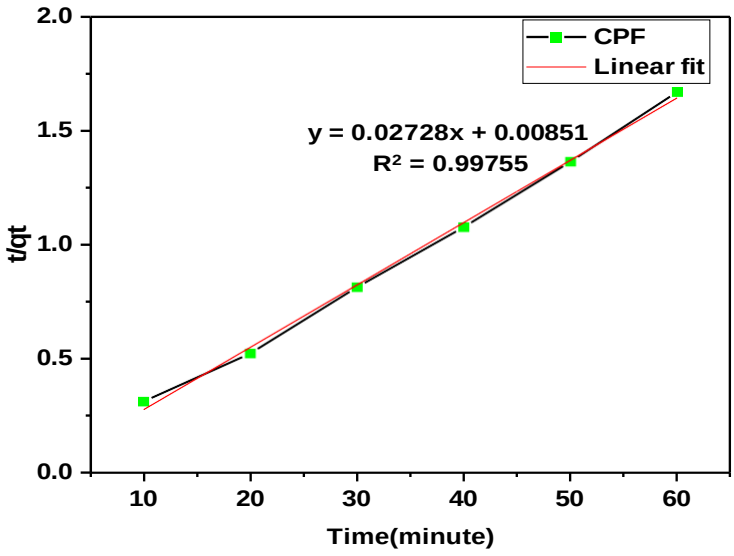

Figure 21:Pseudo-second order kinetic plot for the adsorption of CPF pesticides onto activated bentonite adsorbent

4.6. Regeneration and reusability result

The reusability assessment was executed to give a view of the regeneration potential of the 5% sodium bicarbonate activated bentonite adsorbent and the water treatment procedure expenses. In this study, four consecutive reuse cycles in optimum conditions were carried out to observe the 5% sodium bicarbonate activated bentonite adsorbent's regeneration after chlorpyrifos pesticides adsorption. The desorption experiment of chlorpyrifos pesticides was done as follows. After chlorpyrifos pesticides adsorption by 5% sodium bicarbonate activated bentonite adsorbent in optimum conditions, i.e., 15.0 mL of chlorpyrifos solution volume, 0.03 g of adsorbent dosage, 40 min contact time, solution pH of 6, 100 mg/L initial concentration at an ambient temperature, the activated bentonite adsorbent was poured into 10.0 mL acetonitrile which separated from the solution by effective stirring by using magnetic stirrer bar at 25 °C for 1.5 hr and centrifuge at 3000 rpm for 15 min and then dried in an oven at 95°C to constant mass. The reusability of the regenerated adsorbent was calculated for the above adsorption-desorption experiments four times. In order to assess the possibility of reusing the adsorbent, the percentage of CPF desorbed to adsorb was calculated. Desorption efficiency was calculated by using the equation 17:

$$Desorption\ efficiency = \frac{C - desorbed}{C - adsorbed} \times 100 \ldots\ldots\ldots\ldots\ldots\ldots\ldots\ldots\ldots\ldots Eq.\ 17$$

Where C-desorbed is the amount of the chlorpyrifos insecticides that was removed from the loaded powder after desorption study, adsorbed is $C_0 - Ce$ for each recovery process, C_0 is the initial chlorpyrifos concentration, and Ce is the equilibrium chlorpyrifos concentration in mg/L (Beigi et al., 2023, Hamadeen et al., 2021). The recovery of the adsorbent using acetonitrile was done four times and investigated the degree of adsorption (Beigi et al., 2023, Hamadeen et al., 2021). To investigate the degree of adsorption of the recycled adsorbent after batch adsorption experiment, the filtrate was analyzed by a high performance liquid chromatography system. The results (Figure. 22) showed that the adsorption percentage of chlorpyrifos was calculated using Equations (15) and adsorption percentages of the cycles gradually decreased from 96.57 % to 85.80 %.

Table 10: Reusability of activated bentonite adsorbent for chlorpyrifos pesticides removal.

Cycle	Co(mg/L)	Ce(mg/L)	% Removal
1	51.04	1.75	96.57
2	51.04	3.56	93.02
3	51.04	5.84	88.56
4	51.04	7.76	85.80

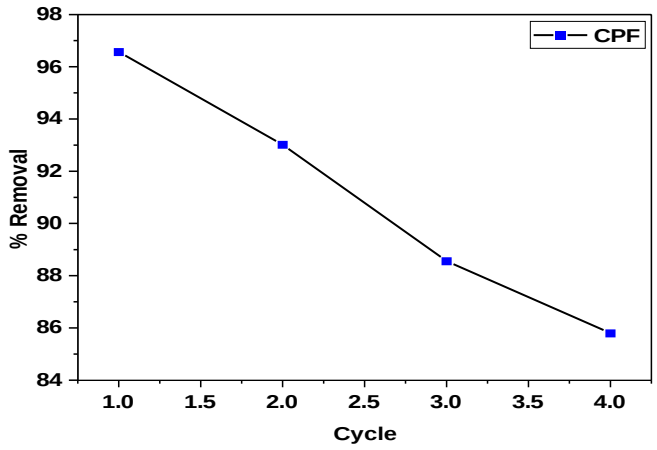

Figure 22: **Reusability** of activated bentonite adsorbent for chlorpyrifos pesticide removal.

4.7. Real sample adsorption study of activated bentonite adsorbents.

To study the chlorpyrifos removal efficiency of the activated bentonite adsorbent, 50 mL sample from wastewater treatment pond of APPF plant were collected at five point of the construction i.e. from all four corners and at the center of the pond treatment into 250 ml volumetric flask. After all the factors that influence chlorpyrifos pesticides adsorption were optimized, such as adsorbent dosage, contact time, and pH of the solution. At the end of the adsorption period, each solution was filtered and then analyzed for chlorpyrifos equilibrium by using HPLC equipped with a UV -Vis detector system. As shown in Table 11 the initial concentration of chlorpyrifos detected in the wastewater sample from treatment pond was 0.974mg/L. The wastewater samples collected, and the chlorpyrifos contents were fed into batch removal adsorption through 5% sodium bicarbonate activated bentonite adsorbents and their adsorption efficiencies were calculated. Real sample application of the activated bentonite adsorbents that chlorpyrifos can be removed by using activated bentonite adsorbents which activated by using sodium bicarbonate has maximum removal efficiencies 90.76% w/w of chlorpyrifos insecticides.

Table 11: Adsorption studies on removal of chlorpyrifos from real wastewater sample

Wastewater sample pollutant	Co(mg/L)	Dose of adsorbent(g/L)	pH	Contact time(min)	Ce(mg/L)	% Removal
CPF	0.974	0.03	6	40	0.09	90.76

The removal efficiency of CPF was about 97.8% in spiked HPLC grade water with batch study. But as shown in the above table 11 slightly lower adsorption percent was obtained for the contaminated wastewater treatment pond of APPF plant 90.76% and similar result was found (Hamadeen et al., 2021) compared to CPF spiked in HPLC grade water adsorption 97.8% as these matrices are more complex than CPF which was spiked into HPLC grade water. And there were other pesticides matrices which compete for the active site of the 5% sodium bicarbonate activate bentonite adsorbent.

5. CONCLUSION AND RECOMMENDATION

5.1. Conclusion

Pesticides like chlorpyrifos, is organic pollutant of water that cause a health risk on aquatic animals, plants, and humans because of its environmental persistence, toxicity and non-biodegradable nature, as well as bioaccumulation of its degraded product. In this work natural bentonite adsorbent was activated by sodium bicarbonate, to investigate the activated bentonite adsorbent efficiency for chlorpyrifos removal from water. The preliminary adsorption capacity results showed that 5% sodium bicarbonate activated bentonite has been successfully applied as promising adsorbent for the removal of selected organophosphorus pesticide, specifically chlorpyrifos from aqueous solutions. The removal and extraction efficiency of 5% sodium bicarbonate activated bentonite adsorbent were improved by adjusting factors including pH, adsorbent dose, adsorption contact time, and adsorbate concentration. The findings indicated that pH 6, an absorption time 40 min, an adsorbent dose 2 g/L, and an initial concentration of 100 mg/L chlorpyrifos. The equilibrium data were modeled by two isotherm equations. Among both, the Langmuir isotherm gave a better fit to the sorption equilibrium data according to the R^2 value, which shows homogeneity of the sorption process. The surface adsorption process aligns with the pseudo second-order model. The analyte's adsorption on the activated bentonite was thus accomplished through chemical adsorption. As this study was performed with laboratory-made solutions to apply this activated bentonite in the treatment of chlorpyrifos-contaminated real water samples for practical applications can be used successfully for the APPF wastewater treatment pond of chlorpyrifos-contaminated sites.

5.2. Recommendations

For the treatment of water polluted with different types of pesticides, many technologies have been evaluated including adsorption methods. Adsorption method has received increasing attention as an efficient, inexpensive and environmentally friendly approach to clean up chlorpyrifos and other pesticide polluted environments. If some further research work is carried out to explore the potential of 5% sodium bicarbonate activated bentonite adsorbent clays, for the removal chlorpyrifos from water body recommended studies are listed below:

- Since effects of other parameters such as activation time, and agitation speed were not studied in the activation studies, it is recommended that these parameters get studied even though their effects as compared to the others is less as observed in literature reviews.
- It is recommended to perform preliminary chlorpyrifos existence study in all water reservoirs and design, economic feasibility study and
- Establish economic scale for 5% sodium bicarbonate activated bentonite manufacturing unit.

6. References

Abdullahi, S. L., & Audu, A. A. (2017). Comparative analysis on chemical composition of bentonite clays obtained from Ashaka and tango deposits in Gombe State, Nigeria. *ChemSearch Journal*, *8*(2), 35-40–40.

Amrety, M. El, Mossad, M., & Fouad, M. (2018). *Removal of Chlorpyrifos from aqueous solution using Electrocoagulation 43*(1), 10 - 15.

Anupam, K., Dhiman, J., Goley, P. K., Anupriya, Pundir, A. S., Yadav, V., & Karri, R. R. (2022). Technologies for pesticide removal from water and wastewater— A bibliometric survey. *Pesticides Remediation Technologies from Water and Wastewater*, *March 2023*, 77–95. https://doi.org/10.1016/B978-0-323-90893-1.00004-0

Ascensão, G., Bernardo, E., & Ferreira, V. M. (2022). An Investigation on the Synthesis of Alkali Activated Materials from Thermally Modified Clays. *Applied Sciences (Switzerland)*, *12*(18). https://doi.org/10.3390/app12189085

Baharum, N. A., Nasir, H. M., Ishak, M. Y., Isa, N. M., Hassan, M. A., & Aris, A. Z. (2020). Highly efficient removal of diazinon pesticide from aqueous solutions by using coconut shell-modified biochar. *Arabian Journal of Chemistry*, *13*(7), 6106–6121. https://doi.org/10.1016/j.arabjc.2020.05.011

Beigi, P., Ganjali, F., Hassanzadeh-Afruzi, F., Salehi, M. M., & Maleki, A. (2023). Enhancement of adsorption efficiency of crystal violet and chlorpyrifos onto pectin hydrogel@Fe3O4-bentonite as a versatile nanoadsorbent. *Scientific Reports*, *13*(1), 1–20. https://doi.org/10.1038/s41598-023-38005-z

Bokulić Petrić, A., Stipičević, S., & Mešić, A. (2023). Stability of malathion, diazinon and chlorpyrifos in different water types – a review. *Journal of Central European Agriculture*, *24*(4), 873–887. https://doi.org/10.5513/JCEA01/24.4.3920

Cuevas, J., Cabrera, M. Á., Fernández, C., Mota-Heredia, C., Fernández, R., Torres, E., Turrero, M. J., & Ruiz, A. I. (2022). Bentonite Powder XRD Quantitative Analysis Using Rietveld Refinement: Revisiting and Updating Bulk Semiquantitative Mineralogical Compositions. *Minerals*, *12*(6). https://doi.org/10.3390/min12060772

Debebe, Y., Alemayehu, E., Worku, Z., Bae, W., & Lennartz, B. (2023). Sorption of 2,4-Dichlorophenoxyacetic Acid from Agricultural Leachate Using Termite Mound Soil: Optimization Using Response Surface Methodology. *Water (Switzerland)*, *15*(2). https://doi.org/10.3390/w15020327

Derbalah, A., Ismail, A., & Shaheen, S. (2013). Monitoring of organophosphorus pesticides and remediation technologies of the frequently detected compound (chlorpyrifos) in drinking water. *Polish Journal of Chemical Technology*, *15*(3), 25–34. https://doi.org/10.2478/pjct-2013-0040

Elzakey, E. M., El-Sabbagh, S. M., Eldeen, E. E. S. N., Adss, I. A. A., & Nassar, A. M. K. (2023). Bioremediation of chlorpyrifos residues using some indigenous species of bacteria and fungi in wastewater. *Environmental Monitoring and Assessment*, *195*(6). https://doi.org/10.1007/s10661-023-11341-3

Farghali, R. A., Basiony, M. S., Gaber, S. E., Ibrahim, H., & Elshehy, E. A. (2020). Adsorption of organochlorine pesticides on modified porous Al30/bentonite: Kinetic and thermodynamic studies. *Arabian Journal of Chemistry*, *13*(8), 6730–6740. https://doi.org/10.1016/j.arabjc.2020.06.027

Fisseha Advisor, K., Tekola, B., & Ababa, A. (2017). *Modification of Bentonite Clay for Adsorption Enhancement for Congo Red Dye Removal from Textile Waste Water*.

Fosu-Mensah, B. Y., Okoffo, E. D., Darko, G., & Gordon, C. (2016). Organophosphorus pesticide residues in soils and drinking water sources from cocoa producing areas in Ghana. *Environmental Systems Research*, *5*(1). https://doi.org/10.1186/s40068-016-0063-4

Hamadeen, H. M., Elkhatib, E. A., Badawy, M. E. I., & Abdelgaleil, S. A. M. (2021). Novel low cost nanoparticles for enhanced removal of chlorpyrifos from wastewater: Sorption kinetics, and mechanistic studies. *Arabian Journal of Chemistry*, *14*(3), 102981. https://doi.org/10.1016/j.arabjc.2020.102981

Hossain, M. S., Chowdhury, M. A. Z., Pramanik, M. K., Rahman, M. A., Fakhruddin, A. N. M., & Alam, M. K. (2015). Determination of selected pesticides in water samples adjacent to agricultural fields and removal of organophosphorus insecticide chlorpyrifos using soil

bacterial isolates. *Applied Water Science*, *5*(2), 171–179. https://doi.org/10.1007/s13201-014-0178-6

HSE. (2018). Pesticides in drinking water: Frequently Asked Questions. *Health Service Executive, National Drinking Water Group*, 10.

Hui, T. J., Ariffin, M. M., & Tahir, N. M. (2010). HYDROLYSIS OF CHLORPYRIFOS IN AQUEOUS SOLUTIONS AT DIFFERENT TEMPERATURES AND pH (Hidrolisis Klorpirifos dalam Larutan Akueus pada Suhu dan pH Berbeza). *The Malaysian Journal of Analytical Sciences*, *14*(2), 50–55.

Hussain, A., & Asi, M. R. (2008). Pesticides as water pollutants. *Groundwater for Sustainable Development: Problems, Perspectives and Challenges*, *September*, 95–101. https://doi.org/10.4018/978-1-5225-6111-8.ch001

Ivanova, N., Gugleva, V., Dobreva, M., Pehlivanov, I., Stefanov, S., & Andonova, V. (2016). We are IntechOpen , the world ' s leading publisher of Open Access books Built by scientists , for scientists TOP 1 %. *Intech*, *i*(tourism), 13.

Jemal, T., Astatke, H., Terfe, A., & Mekonen, S. (2023). Effect of conventional and household water treatment technologies on the removal of pesticide residues in drinking water, Jimma town, Southwestern, Ethiopia. *PLoS ONE*, *18*(7 July), 1–18. https://doi.org/10.1371/journal.pone.0288086

Johnson, S., & Kumar, A. (2015). *ANALYSIS OF PESTICIDE RESIDUES*. *January 2006*.

Joint FAO/IAEA Division of Nuclear Techniques in Food and Agriculture., & International Atomic Energy Agency. (2009). *Quality control of pesticide products* (Issue July).

Joshi, V., Jindal, M. K., & Sar, S. K. (2023). Approaching a discussion on the detachment of chlorpyrifos in contaminated water using different leaves and peels as bio adsorbents. *Scientific Reports*, *13*(1), 1–20. https://doi.org/10.1038/s41598-023-38471-5

Kamalanathan, I. (2016). *Chlorpyrifos Removal for Wastewater Reuse*. https://scholarworks.uark.edu/cgi/viewcontent.cgi?referer=https://www.google.com/&httpsredir=1&article=1096&context=cheguht

Khalifa, A. Z., Cizer, Ö., Pontikes, Y., Heath, A., Patureau, P., Bernal, S. A., & Marsh, A. T. M. (2020). Advances in alkali-activation of clay minerals. *Cement and Concrete Research*, *132*(March), 106050. https://doi.org/10.1016/j.cemconres.2020.106050

Kiviranta, L., & Kumpulainen, S. (2011). Quality control and characterization of bentonite materials. *POSIVA Report*, *December*, 102. http://www.iaea.org/inis/collection/NCLCollectionStore/_Public/43/108/43108887.pdf

Köck-Schulmeyer, M., Villagrasa, M., López de Alda, M., Céspedes-Sánchez, R., Ventura, F., & Barceló, D. (2013). Occurrence and behavior of pesticides in wastewater treatment plants and their environmental impact. *Science of the Total Environment*, *458–460*, 466–476. https://doi.org/10.1016/j.scitotenv.2013.04.010

Kumar, P., Arshad, M., Gacem, A., Soni, S., Singh, S., Kumar, M., Yadav, V. K., Tariq, M., Kumar, R., Shah, D., Wanale, S. G., Al Mesfer, M. K. M., Bhutto, J. K., & Yadav, K. K. (2023). Insight into the environmental fate, hazard, detection, and sustainable degradation technologies of chlorpyrifos—an organophosphorus pesticide. *Environmental Science and Pollution Research*, *30*(50), 108347–108369. https://doi.org/10.1007/s11356-023-30049-y

Leena, S. (2017). *Activation of Raw Bentonite (Afar Region) Using Sulfuric Acid for Rapeseed and Niger Seed Oil Bleaching and*. 1–103.

Maged, A., Kharbish, S., Ismael, I. S., & Bhatnagar, A. (2020). Characterization of activated bentonite clay mineral and the mechanisms underlying its sorption for ciprofloxacin from aqueous solution. *Environmental Science and Pollution Research*, *27*(26), 32980–32997. https://doi.org/10.1007/s11356-020-09267-1

Majumder, R. (2022). Effects of Aquatic Vegetation and Water Turbidity on Chlorpyrifos-Induced Mortality of Nile Tilapia Oreochromis niloticus. *Journal of Fisheries and Environment*, *46*(2), 47–57.

Obiageli, A. R. (2017). ADSROPTION OF CATIONIC DYE ONTO LOW-COST ADSORBENT SYNTHESIZED FROM BENTONITE CLAY Part I. KINETIC AND THERMODYNAMIC STUDIES. *Journal of Chemical Technology and Metallurgy*, *52*, 491–504.

Pluangklang, C., & Rangsriwatananon, K. (2021). Article facile method by bentonite treated with heat and acid to enhance pesticide adsorption. *Applied Sciences (Switzerland), 11*(11). https://doi.org/10.3390/app11115147

Qurie, M., Khamis, M., Ayyad, I., Scrano, L., Lelario, F., Bufo, S. A., Mecca, G., & Karaman, R. (2016). Removal of chlorpyrifos using micelle–clay complex and advanced treatment technology. *Desalination and Water Treatment*, *57*(33), 15687–15696. https://doi.org/10.1080/19443994.2015.1096836

Saleh, I. A., Zouari, N., & Al-Ghouti, M. A. (2020). Removal of pesticides from water and wastewater: Chemical, physical and biological treatment approaches. In *Environmental Technology and Innovation* (Vol. 19). Elsevier B.V. https://doi.org/10.1016/j.eti.2020.101026

Saleh, S. K., & Mahasneh, M. A. (2015). Activation of Jordanian Ore Bentonite by Sodium Carbonates. *Journal of Minerals and Materials Characterization and Engineering*, *03*(06), 477–487. https://doi.org/10.4236/jmmce.2015.36050

Samadi-Maybodi, A., Ghezel-Sofla, H., & BiParva, P. (2023). Simultaneous removal of phenoxy herbicides, 2-methyl-4-chlorophenoxyacetic acid and 2,4-dichlorophenoxyacetic acid from aqueous media by magnetized MgAl-LDH@Fe3O4 composite: application of partial least squares and Doehlert experimental design. *Journal of Environmental Health Science and Engineering*. https://doi.org/10.1007/s40201-023-00877-8

Senthilkumaar, S., Krishna, S. K., Kalaamani, P., Subburamaan, C. V., Ganapathy Subramaniam, N., & Kang, T. W. (2010). Kinetic approach for the adsorption of organophosphorous pesticides from aqueous solution using “waste” jute fiber carbon. *E-Journal of Chemistry*, *7*(SUPPL. 1). https://doi.org/10.1155/2010/947070

Shattar, S. F. A., Zakaria, N. A., & Foo, K. Y. (2020). One step acid activation of bentonite derived adsorbent for the effective remediation of the new generation of industrial pesticides. *Scientific Reports*, *10*(1), 1–13. https://doi.org/10.1038/s41598-020-76723-w

Sishu, F. K., Tilahun, S. A., Schmitter, P., Assefa, G., & Steenhuis, T. S. (2022). Pesticide Contamination of Surface and Groundwater in an Ethiopian Highlands’ Watershed. *Water (Switzerland)*, *14*(21), 1–20. https://doi.org/10.3390/w14213446

Suciu, N. A., & Capri, E. (2009). Adsorption of chlorpyrifos, penconazole and metalaxyl from aqueous solution by modified clays. *Journal of Environmental Science and Health - Part B Pesticides, Food Contaminants, and Agricultural Wastes*, *44*(6), 525–532. https://doi.org/10.1080/03601230902997543

T. Al Hattab, M., & E. Ghaly, A. (2012). Disposal and Treatment Methods for Pesticide Containing Wastewaters: Critical Review and Comparative Analysis. *Journal of Environmental Protection*, *03*(05), 431–453. https://doi.org/10.4236/jep.2012.35054

Tadesse, S. H. (2022). Application of Ethiopian bentonite for water treatment containing zinc. *Emerging Contaminants*, *8*, 113–122. https://doi.org/10.1016/j.emcon.2022.02.002

Tole, I., Habermehl-Cwirzen, K., & Cwirzen, A. (2019). Mechanochemical activation of natural clay minerals: an alternative to produce sustainable cementitious binders – review. *Mineralogy and Petrology*, *113*(4), 449–462. https://doi.org/10.1007/s00710-019-00666-y

Unnithan, R. R., & Soorya, S. R. (2017). Characterization of Na2CO3 activated Calcium Bentonite and its application as a GCL. *International Journal of Engineering Research & Technology (IJERT)*, *5*(8), 1–4.

Velkoska-Markovska, L., Petanovska-Ilievska, B., & Markovski, A. (2018). Application of High Performance Liquid Chromatography to the Analysis of Pesticide Residues in Apple Juice. *Contemporary Agriculture*, *67*(1), 93–102. https://doi.org/10.2478/contagri-2018-0014

Wang, C., Liu, B., Xu, D., Zhang, D., He, F., Zhou, Q., & Wu, Z. (2017). Mitigation of wastewater-borne chlorpyrifos in constructed wetlands: The role of vegetation on partitioning. *Polish Journal of Environmental Studies*, *26*(1), 347–354. https://doi.org/10.15244/pjoes/64375

Wasse Bekele, G., & Fernandez, N. (2014a). Removal of nitrate ion from aqueous solution by modified Ethiopian bentonite clay. *International Journal of Research in Pharmacy and Chemistry*, *4*(1), 192–201.

Wasse Bekele, G., & Fernandez, N. (2014b). Removal of nitrate ion from aqueous solution by modified Ethiopian bentonite clay. *International Journal of Research in Pharmacy and*

Chemistry, *4*(1), 192–201. www.ijrpc.com

World Health Organization. (2004). Chlorpyrifos in Drinking-water. *Background Document for Development of WHO Guidelines for Drinking-Water Quality.*, 14.

Zhang, H., Zhou, J., Muhammad, Y., Tang, R., Liu, K., Zhu, Y., & Tong, Z. (2019). Citric acid modified bentonite for congo red adsorption. *Frontiers in Materials*, *6*(February), 1–11. https://doi.org/10.3389/fmats.2019.00005

Appendix

Appendix-1: **The preliminary adsorption capacity results**.

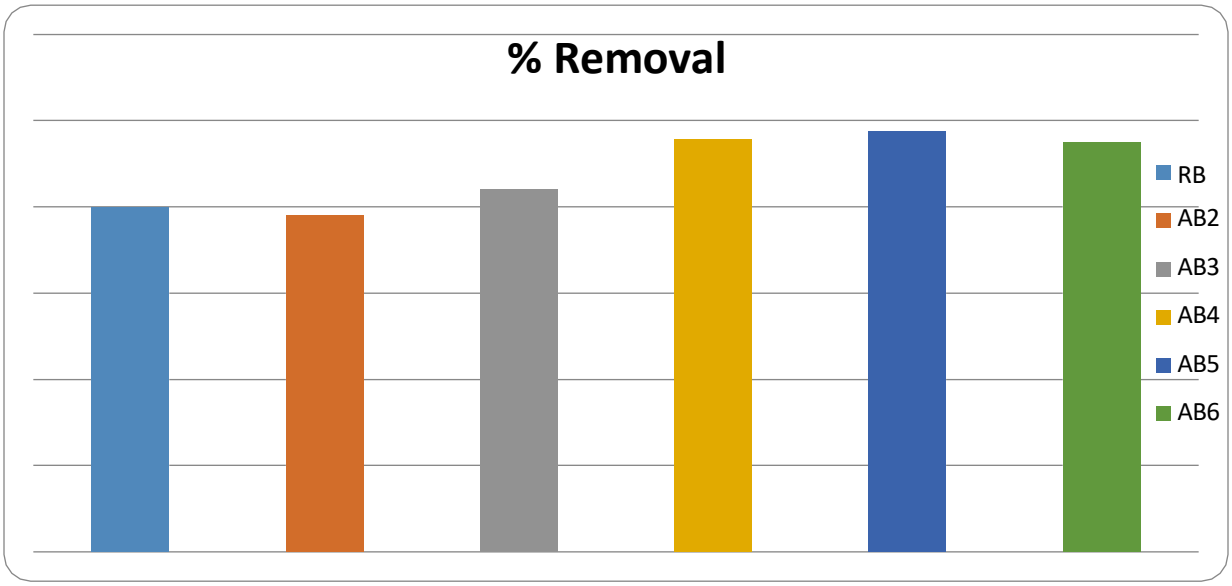

Appendix-2: **data of percent recoveries of calibration curve**

S/NO	CM(ppm),	Peak area	CE(ppm)	Percent Recovery(Q)
1	0.015	833.85	0.0139	92.67
2	0.02	1106.24	0.017	85
3	0.025	1439.21	0.023	92
4	0.03	1896.01	0.029	96.67
5	0.035	2526.48	0.033	94.30